ELECTROLYTIC DEPOSITION OF MgO ON STAINLESS STEEL SUBSTRATE

A Thesis Submitted to the College of

Graduate Studies and Research

In Partial Fulfillment of the Requirements

For the Degree of Master of Science

In the Department of Mechanical Engineering

University of Saskatchewan

Saskatoon

By

Siyamak Javadian

Permission to Use

In presenting this thesis in partial fulfillment of the requirements for a Postgraduate degree from the University of Saskatchewan, I agree that the Libraries of this University may make it freely available for inspection. I further agree that permission for copying of this thesis in any manner, in whole or in part, for scholarly purposes may be granted by the professor or professors who supervised my thesis work or, in their absence, by the Head of the Department or the Dean of the College in which my thesis work was done. It is understood that any copying or publication or use of this thesis or parts thereof for financial gain shall not be allowed without my written permission. It is also understood that due recognition shall be given to me and to the University of Saskatchewan in any scholarly use which may be made of any material in my thesis.

Disclaimer

The University of Saskatchewan were exclusively created to meet the thesis and exhibition requirements for the degree of Master of Science at the University of Saskatchewan. Reference in this thesis to any specific commercial products, process, or service by trade name, trademark, manufacturer, or otherwise, does not constitute or imply its endorsement, recommendation, or favouring by the University of Saskatchewan. The views and opinions of the author expressed herein do not state or reflect those of the University of Saskatchewan, and shall not be used for advertising or product endorsement purposes.

Requests for permission to copy or to make other use of material in this thesis in whole or part should be addressed to:

Head of the Department of Mechanical Engineering
University of Saskatchewan
Saskatoon, Saskatchewan (S7N 5A9)

ABSTRACT

The main objective of this thesis was to fabricate and characterize magnesium oxide coating on stainless steel alloy (SAE 316L). Electrolytic processing, followed by sintering was used for making it. Coating the heater tubes used in refinery industry with magnesium oxide is expected to increase the oxidation and corrosion resistance of the tubes. Fabrication of magnesium oxide coating was a two-step process. First, a magnesium hydroxide coating was deposited on the SAE 316L stainless steel substrate in an electrochemical bath and then the magnesium hydroxide was converted to magnesium oxide during sintering. The substrate was electropolished in a 15% sulfuric acid solution before immersing in the electrochemical bath.

Electrolytic processing parameters such as deposition time and voltage were optimized and others like the distance between anode and cathode, concentration of magnesium ions in the solution and the surface area of the cathode and the anode were kept constant. The microstructure and texture of the magnesium hydroxide coating was analyzed using scanning electron microscopy (SEM) and X-ray diffraction (XRD). Sintering parameters were also optimized. Corrosion and oxidation resistance of the fabricated coating were compared to that of the uncoated sample in both high and room temperature. The hardness of the magnesium oxide coating was measured using a nano-hardness tester. The developed coating has uniform and crack free surface.

ACKNOWLEDGEMENTS

I would like to express my deep gratitude to my supervisors, Professor J. A. Szpunar. Thank you for your guidance and encouragement throughout this research. Without your support, leadership, and friendship this work would not have been possible.

I would also like to express my appreciation to my committee members Professor Oguocha and Professor Odeshi whom have provided me with guidance and encouragement throughout my Master's studies.

I would like to thank UOP LLC Honeywell Company for their financial support of this project.

I am also grateful to the following people for contributing towards the completion of this work:

- Mr. Rob Peace for providing me with the materials and equipment.
- My dear friend, Ahmad Lajevardi for his help in the corrosion tests. Salman Razavi, Hamed Akhiani, Majid Nezakat and Nilesh Gurao for their useful comments throughout this project, Ming Song for his kind helps in sample preparation and all members of the research group for providing a friendly working environment.
- Mick Ellis for editing the thesis.
- University of Saskatchewan and department of mechanical engineering for providing the research facilities.

DEDICATION

I dedicate this thesis to my parents.

Thank you very much for your love and encouragement throughout my life.

TABLE OF CONTENTS

LIST OF TABLES

LIST OF FIGURES

NOMENCLATURE

Acronyms

CVD	Chemical Vapor Deposition
EDS	Energy-Dispersive X-ray Spectroscopy
ELD	Electrolytic Deposition
EPD	Electrophoretic Deposition
FCC	Face Center Cubic
FGM	Functionally Graded Materials
HCP	Hexagonal Close-Packed
IPF	Inverse Pole Figure
mpy	milli-inch per year
PF	Pole Figure
PVD	Physical Vapor Deposition
SS	Stainless Steel
TBC	Thermal Barrier Coating
UHTC	Ultra High Temperature Ceramic
Eoc	Open Circuit Voltage

English Symbols

E	potential
i	current
A	ampere
n	nano
cm	centimeter
℃	centigrade
q_S	charge in solution

q_M	charge on metal surface
V	voltage
b_a	anodic Beta Tafel constant
b_c	cathodic Beta Tafel constant

Greek Symbols

μ	micron
η	over potential

CHAPTER 1

INTRODUCTION

1.1 Ceramic Coatings

Coatings are used to increase the performance of materials by isolating the base material from the environment of a service atmosphere [1]. Among various coating materials, ceramics are often used because of their high melting temperature. Materials for high temperature applications are gaining increased interest in high-tech industries. Gas turbines, heater tubes and turbine blades are some of these applications. Although some alloys such as high chromium and nickel stainless steels and nickel based super alloys can tolerate high temperatures, ceramics are better choice in applications where high temperature oxidation and corrosion are expected. In such corrosive environments, ceramics are best choice because of their high melting temperature, good corrosion resistance and low thermal conductivity, which make them candidates for thermal barrier coatings (TBCs). However, ceramics have a big drawback which is their low ductility [2].

Ryan Aeronautical Company is one of the pioneers of the successful application of ceramic coating on metals where they coated the exhaust header of Boeing airplanes with ceramics, test it on actual flights, and observe the increase of the lifetime of the exhaust headers. In fact the ceramic coating protects the metallic substrate from oxidation, corrosion and other high temperature phenomena, which can deteriorate the metallic exhaust header. Application of ceramic coating not only extends the life-time of the engine parts in airplanes but also makes it possible to use less expensive materials such as SS321 alloy instead of nickel rich alloys [3].

Thermal barrier coating is one of the common applications of ceramics that has been developed in recent years. TBC is a thin layer of ceramic coating which has low thermal conductivity and, as a result, less heat is conducted to the substrate. The major issue in TBCs is the spallation of the ceramic coating during thermal exposure that results from a mismatch of the thermal expansion of the coating and the metallic substrate. Functionally graded materials

(FGM) have been recently introduced to overcome this problem. In FGM the structure or composition of the coating layers gradually changes to reduce thermal shocks when moving from the substrate to the coating [4]. Ceramic coatings are also candidates for ultra-high temperature applications; these are called ultra-high temperature ceramics (UHTC). The application is in aircraft engines where speeds exceed the speed of sound and the temperature of some engine parts exceeds 2500^{o}C [5].

A common method for applying ceramic coatings on metallic substrates is thermal plasma spray in which ceramic powders are deposited at high temperature and speed. In this method the powder is heated to be soft enough and then gas pressure is used to accelerate the particles towards the substrate producing a coating [6]. However among the common ceramic coating methods such as PVD, CVD, Sol-Gel and others [6], electrochemical methods including electrolytic deposition and electrophoretic deposition are of special interest due to their low cost, simplicity and the ability to coat complicated shapes [7]. Electrolytic and electrophoretic processing of different ceramic coatings on metals is reported [8-42]. Although there are a few reports available in the open literature on the electrolytic processing of magnesium oxide [11 and 12], no mechanical and corrosion properties are reported.

1.2 Motivation

Application of MgO is in heater tubes in refinery industry or any power plant which works with fossil fuels. Figure 1.1 schematically represents different parts of a power station. Combustion of fossil fuels releases fly ash which contains sulfur compounds. This product combines with the heater tube material and forms low melting temperature compounds that remove the protective oxide layer on the surface of steel or stainless steel and leads to deterioration of the tubes in a shorter period. Magnesium oxide is able to react with sulfur and other substances in the ash to create high melting temperature compound that prevents the removal of protective oxide layer [43]. Magnesium oxide powder is conventionally added to the fuel before combustion, injected to the combustion zone, or directly applied to the area of corrosion occurs in order to mitigate fuel ash corrosion [44]. However, using the MgO powder in the improvement of corrosion resistance of the tubes is not very significant and a lot of magnesium oxide is wasted. By electrolytically coating the fireside of the heater tubes with

magnesium oxide less magnesium oxide will be consumed and the lifetime of the tubes can be extended.

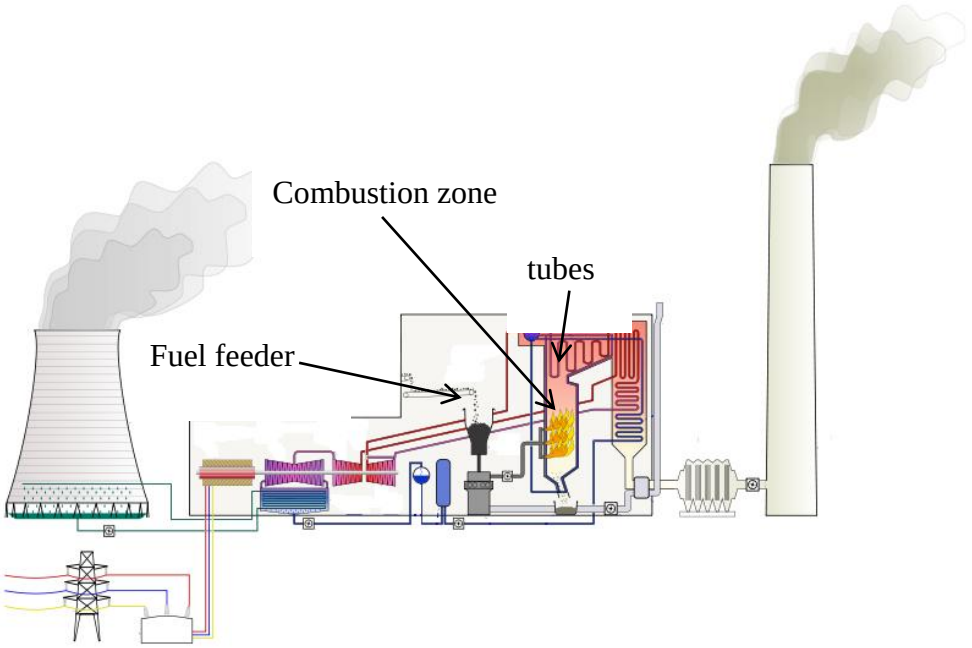

Figure 1.1 Schematic drawing of a power station working with fossil fuel [45].

1.3 Thesis Objectives

The main objectives of this project are listed below:

1. To fabricate a magnesium oxide coating on SAE 316L stainless steel by electrochemical methods.
2. To optimize electrolytic deposition and sintering parameters.
3. To optimize the microstructure of the coating before and after sintering.
4. To evaluate the mechanical and corrosion properties of the coating.

1.4 Thesis Outlines

In the chapter 2 of this thesis, the fundamentals of electrochemical deposition and the parameters affecting the processing of coating will be discussed. Some of the applications of magnesium oxide and hydroxide will be mentioned. At the end of this chapter the previous works done on electrolytic processing of magnesium hydroxide is reported. Chapter 3 includes a detailed description of the material used in the experiment and the experimental procedures.

Chapter 4 is dedicated to results and discussion, which is divided into two sections. In the first section the results of different characterization tests of magnesium hydroxide coating including XRD and SEM are presented. In the magnesium oxide section, the results of microstructural characterization of the coating after sintering are discussed and the results of the room and high temperature corrosion, oxidation and mechanical tests are presented. Finally in chapter 5, conclusions of the thesis and recommendation for future investigation are presented.

CHAPTER 2

ELECTROCHEMICAL DEPOSITION OF CERAMICS

2.1 Overview of Chapter 2

In this chapter, principles of electrolytic deposition including interaction of water molecules with dissolved ions, metal-solution interphase, kinetics of deposition and parameters affecting the microstructure of the coating will be discussed. Various applications of magnesium oxide and hydroxide and results of the previous works on electrolytic processing of magnesium hydroxide are discussed.

2.2 Electrochemical Deposition Methods

Electrochemical methods including electrolytic deposition (ELD) and electrophoretic deposition (EPD) are widely used for making coatings on different substrates. In EPD charged particles are moved by electric filed, towards the cathode and deposited on the substrate to make a uniform film. Further sintering is usually applied to this film to produce a more compact and dense coating. Using EPD for processing of various ceramic films and metallic particles was reported [18-29].

In ELD salts of metals are dissolved in a solution and deposited on the electrode. Using electrochemical methods to deposit ceramics and metals hydroxides has been reported by many researchers [30-42]. A big challenge in making a ceramic coating on a metallic substrate is the adherence of the coating to the substrate. Especially in coating ceramics on stainless steel, the formation of chromium oxide on the surface of the substrate is a big issue. On the one hand this oxide layer protects stainless steel from further oxidation; on the other hand it causes poor adhesion of the coating to the stainless steel substrate. Using a conversion coating between the ceramic coating and metallic substrate can increase the adherence [14-16]. Conversion coating can be a separate layer added between the coating and substrate or a simple pretreatment of the

substrate before applying the ceramic coating in order to remove the chromium oxide layer. Since ELD is used in this project to deposit magnesium hydroxide on a metallic substrate, it will be discussed in more detail in this chapter.

2.3 Principles of Electrolytic Deposition

Cathodic deposition is the most important mechanism in electrolytic deposition in which hydroxides are generated with cathodic reactions and increase the pH of the solution close to the cathode. Metal ions that are more stable in low pH are now available in the solution and will react with the hydroxides beside the cathode where pH is higher and form a hydroxide of the metal that is deposited on the cathode [17].

There are many important elements of electrolytic deposition: the solution, the type of electrodes, interaction of the solution with the cathode, the mechanism of deposition, kinetics of deposition, nucleation and growth of the deposit on the cathode are only some of the parameters that are involved in this process. To fully understand the mechanism of electrolytic deposition, one should understand the structure of solution, the interaction of solution with metal and the motion of ions in the solution towards the cathode. In the following sections the most important aspects of electrolytic deposition will be discussed.

2.3.1 Electrolytic Cell

A typical electrolytic cell is comprised of two electrodes, two multi-meters to measure voltage and amperage and a power supply. A schematic of an electrolytic cell is shown in Figure 2.1. One of the electrodes is the cathode, which is usually the metallic substrate on which the coating will be deposited. The other electrode is the anode, which is usually a bar or rod of graphite or other noble materials such as platinum. Reaction at the anode is oxidation and at the cathode is reduction [46].

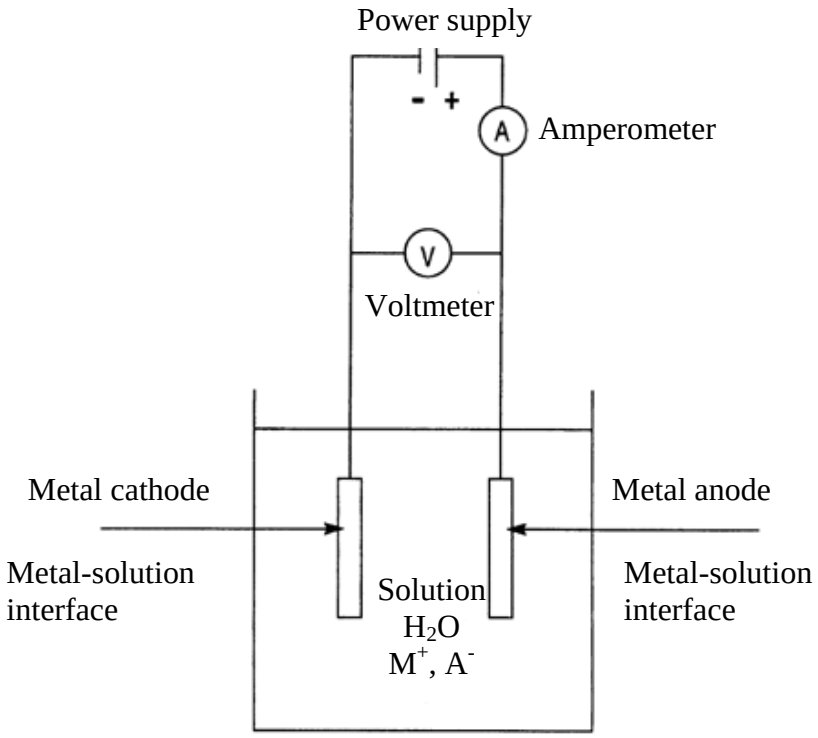

Figure 2.1 Schematic drawing of a typical electrolytic cell used for electrolytic deposition [47], reprinted with permission from the publisher.

2.3.2 Electrolytic Solution

The electrolytic solution is usually composed of water and ionic crystal. Although in some cases alcohols are also added to the solution, in this section it is assumed that the ionic crystal is dissolved just in water. There are different models for the structure of water. In the cluster model, H_2O molecules are considered as clusters of structured and unstructured regions. According to this model pure water breaks up with the following reaction [47]:

$$H_2O \rightarrow H^+ + OH^- \quad (2.1)$$

When ionic crystals MA (like salts of metals) are introduced to this pure water the following reaction occurs [47]:

$$M^{z+}A^{z-} + (m+a)H_2O \rightarrow M^{z+}(mH_2O) + A^{z-}(aH_2O) \quad (2.2)$$

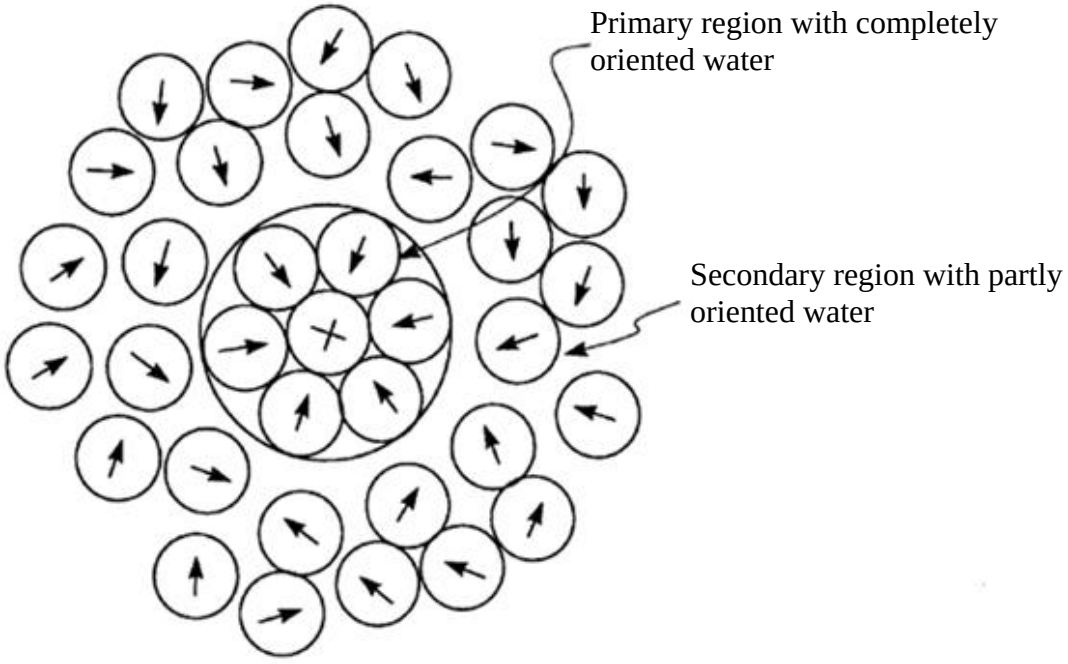

Figure 2.2 Schematic drawing of ion-dipole model showing the interaction of water and ions [47], reprinted with permission from the publisher.

There are different models for the interaction between water and the ionic crystals. In the ion-dipole model it is suggested that water molecules placed themselves around the ions and one end of the water molecule attaches to the ion by electrostatic forces. So a certain number of water molecules is attached to this ion and do not move individually but this complex moves as a unit [47]. Figure 2.2 schematically shows this model. When ions are added to the water, the water clusters breakup and as a result the amount of water molecules present in the cluster will decrease and according to the following equation the dielectric constant of the solution will decrease [47]:

$$\mu_{group}=\mu(1+g\cos\gamma) \qquad (2.3)$$

In this equation, g is the amount of water molecules in the cluster, μ is molecular dipole moment, μ_{group} is group of water molecules dipole moment and γ is the average of the cosines of the angles between dipole moment of the water molecule at the center and the molecules attached to it [47]. A decrease in g means a decrease in μ_{group}. According to [47] dielectric constant (ε) is function of μ_{group} and it decreases when μ_{group} decreases. The value of the dielectric constant is low at the centre (Figure 2.2) and increases while moving away towards the outer layers [47].

2.3.3 Interphase of Metal and Solution

The structure of metals can be described as positive ions covered by free electrons. These free electrons create a dipole layer on the surface. When the metal is immersed in the solution, electron exchange between the solution and metal will occur (Figure 2.3). In an equilibrium state, the number of ions leaving the metal is equal to the number of electrons entering the metal [47].

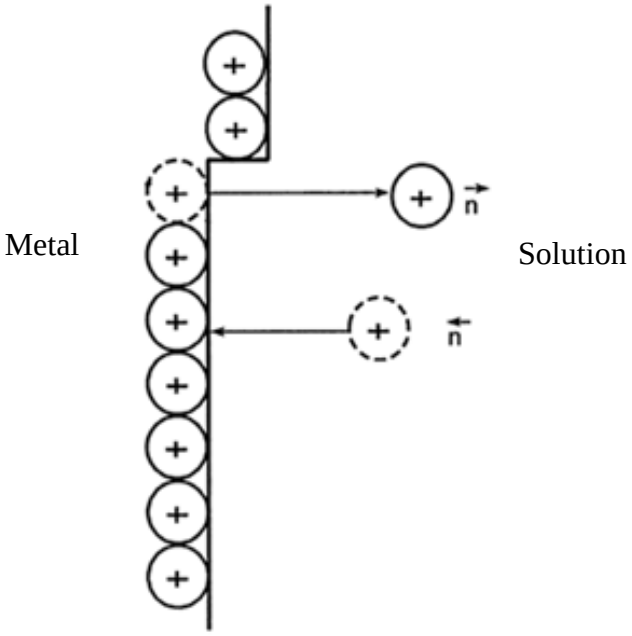

Figure 2.3 Interphase of metal-solution showing that at equilibrium state the number of electrons leaving the solution is equal to the number of electrons entering the solution [47], reprinted with permission from the publisher.

Figure 2.3 shows equilibrium state, but if an extra source of electrons is provided there is no longer equilibrium. In this situation the interaction at the metal-solution interface is described by other models. The simplest is Helmholtz Compact Double-layer model. This model assumes that any extra charge (q_S) in the solution will line up at a certain distance (XHP) from the metal surface. This makes the interphase look like a capacitor where one layer is in the solution with a charge of (q_S) and the other layer (q_M) with an opposite charge is on the metal surface. This structure is called double layer and variation of potential in this region is linear (Figure 2.4) [47].

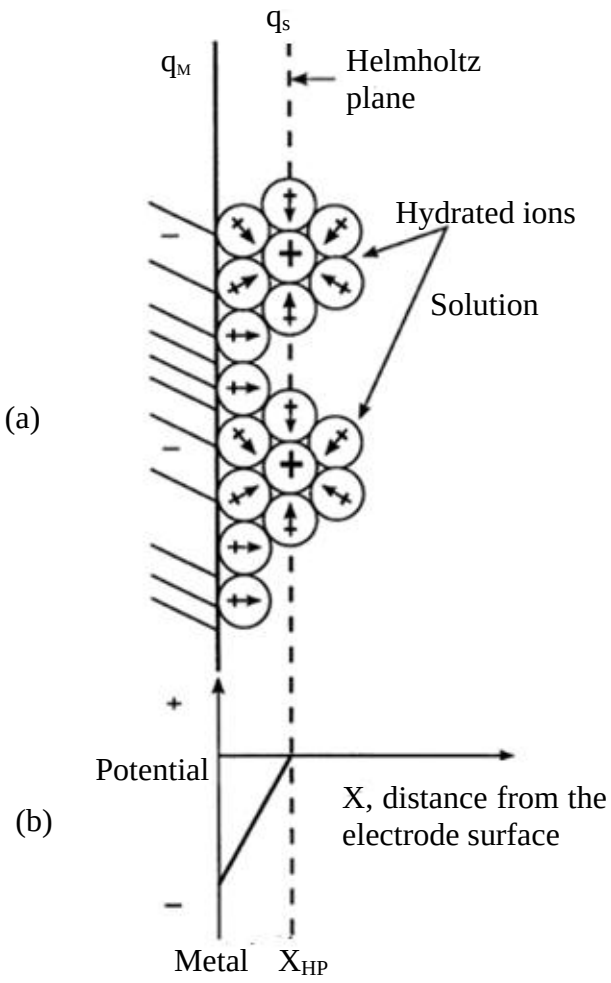

Figure 2.4 (a) Schematic drawing of Helmholtz double layer model showing how the ions are oriented in the double layer when there is non-equilibrium state; (b) showing the linear change of potential in double layer [47], reprinted with permission from the publisher.

2.3.4 Nucleation and growth of Deposits

When an extra charge is applied to the system by a power supply, the potential of the metal (electrode) is different from the equilibrium state. If the potential at equilibrium state is E and the potential due to the charge form power supply is E(I), the over-potential (η) will be [47]:

$$\eta = E(I) - E \tag{2.4}$$

This over-potential influences charge transfer, diffusion, chemical reactions and crystallization. These processes determine the nucleation and growth rate of the deposit [47].

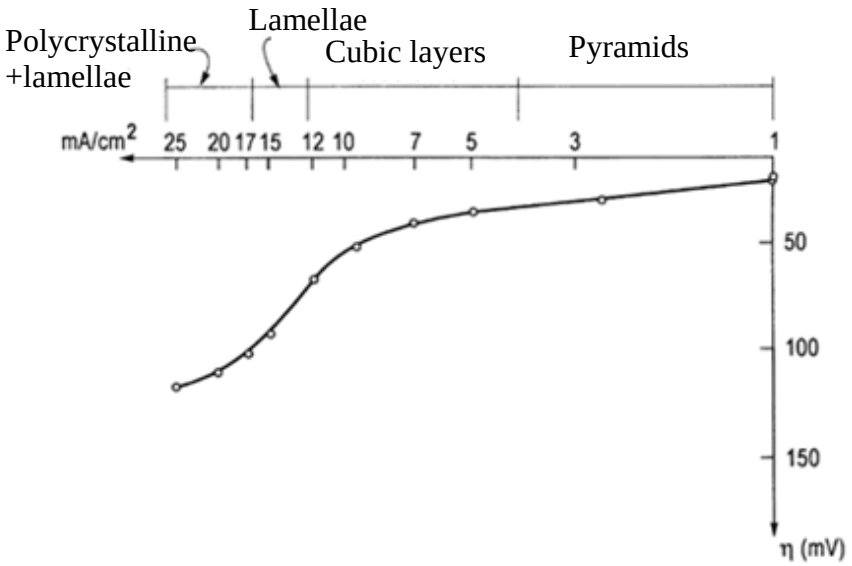

Figure 2.5 Over-potential vs. electric current curve showing that by changing the value of over-potential, the morphology of copper electrodeposits can be significantly changed. The electrolytic solution was $NCuSO_4$ and NH_2SO_4 [47], reprinted from Journal of Electrochimica Acta, Vol. 2, issue 1-3, H. Seiter, H. Fischer, L. Albert Elektrochemisch-morphologische studien zur erforschung des mechanismus der elektrokristallisation, fern vom anfangszustand, pp. 97-120, Copyright (1960), with permission from Elsevier.

Figure 2.5 shows that the magnitude of the over-potential affects the morphology of the deposit. It is worth mentioning that although earlier theories for nucleation consider the metal as a perfect surface where there is no preferable site; in practice surface morphology, texture and interphases influence the nucleation rate and structure of the nuclei [47].

2.3.5 Structure of Electrolytic Deposits

Physical, mechanical, chemical and magnetic properties of a deposit are determined by the structure of the deposit. There are different classifications for the structure of a deposit. One of these classifies the structure of a deposit into five groups [47]:

1. Columnar: This structure is usually observed in compact thin films where there is preferred orientation for growth.

2. Equiaxed: In this structure, the grains have equiaxed shape and are larger compared to a columnar structure grains.
3. Dendritic: This structure can be seen in mass-transfer controlled electrochemical systems.
4. Nodular: This is also known as cauliflower type.
5. Fibrous: This is a non-compact structure.

Among these structures, columnar and equiaxed are compact structures and other structures are non-compact [47]. Each of the morphologies has various applications. While compact structure is an advantage in corrosion and oxidation resistance, non-compact or porous structures are preferred in catalysts because of their higher surface area. Various parameters can affect the structure of the deposits. On the one hand, increasing the metal ion concentration, temperature of the solution and agitation in the solution increases the grain size of the processed coating. On the other hand, adding agents to the solution, increasing current density, and polarization leads to the decrease in the grain size of the processed coating [47].

2.3.6 Texture of Coatings

Each grain in the sample has a crystallographic orientation. If the orientation of crystals in a polycrystalline material is not random, the sample has a preferred orientation. This preferred orientation is known as texture [48]. XRD can be used to measure orientation of selected crystallographic planes and represent the results as a stereographic projection called pole figure of planes. For example, pole figure of (111) plane shows the orientation distribution of the planes in reference frame of the sample. Next step in texture analysis is calculation of the Orientation Distribution Function (ODF) from the measured pole figures, which describes the orientation distribution of the grains in the sample [49]. Resmat software calculates ODF and recalculates the selected planes from the ODF. IPF (Inverse Pole Figure) is opposite of PF. While pole figure shows the orientation distribution of a selected (hkl) plane in the sample reference frame, the inverse pole figure refers to the distribution of the selected direction of the sample in the crystal frame [50]. IPF is also calculated from the ODF in Resmat software.

Analyzing the texture of coatings is an important step in fabrication of a coating for a specific application. The textures of deposits are mainly determined by electrochemical

parameters and to some extend also by substrate properties. Parameters such as current density, pH and over-potential significantly affect the texture of the deposits [47].

2.4 Applications of Magnesium Oxide

One of the most important applications of magnesium oxide is in petrochemical industry. One of the concerns of this industry is dealing with environmentally harmful gaseous emissions such as CO_2, CO, SO and NO_x (greenhouse gases) into the atmosphere and H_2S. A new approach for filtering these gases is to use aerogel filters. Higher surface area is an advantage in such applications. Both magnesium and magnesium hydroxide can act as an absorbent of gases due to the reactions listed in Table 2.1 [51].

Table 2.1 Possible reactions of magnesium oxide and magnesium hydroxide, reprinted from Journal of Applied Thermal Engineering, Vol. 18, Ahmed, M.S., Attia, Y.A, Multi-metal oxide aerogel for capture of pollution gases from air, pp. 787-797, Copyright (1998), with permission from Elsevier.

MgO and $Mg(OH)_2$ reactions	
	$MgO+H_2O=Mg(OH)_2$
Absorption of SO_2	$Mg(OH)_2+SO_2=MgSO_3+H_2O$; $MgSO_3+1/2\ O_2=MgSO_4$
Absorption of CO_2	$Mg(OH)_2+CO_2=MgCO_3+H_2O$
Absorption of CO	$Mg(OH)_2+CO+1/2\ O_2=MgCO_3+H_2O$
Absorption of NO	$Mg(OH)_2+2NO+3/2\ O_2=Mg(NO_3)_2+H_2O$
Absorption of H_2S	$MgO+H_2S=MgS+H_2O$

2.5 Applications of Magnesium Hydroxide

Magnesium hydroxide deposited on magnesium alloys (AZ91) is used to increase the corrosion resistance of the biodegradable materials in biomedical applications such as magnesium alloys (AZ31). It was claimed that the corrosion rate of the coated magnesium alloy (AZ31) samples was lower than non-coated samples immersed in Hank's solution; however the biocompatibility of the coating should be still investigated [52]. Magnesium hydroxide is also used as a flame retardant in the form of the composite or the coating on plastics. Magnesium hydroxide is an acid and halogen free fire retardant. In comparison to aluminum hydroxide, which is conventionally used as a fire retardant, magnesium hydroxide has a higher decomposition temperature, which is 300°C compared to aluminum hydroxide which is 230°C.

Many studies have proved the reduction of smoke emission using magnesium hydroxide as a fire retardant. Actually the endothermic decomposition of magnesium hydroxide at 330°C removes heat from the substrate and lowers the heat available for igniting a fire [53].

2.6 Crystallographic Structure of Magnesium Oxide and Magnesium Hydroxide

Figure 2.6 schematically shows the structure of magnesium oxide. This structure is also known as NaCl type structure [54]. In magnesium oxide (magnesia), Mg^{2+} ions occupy FCC sites and O^- takes octahedral sites [55]. Figure 2.7 shows crystallographic structure of magnesium hydroxide where Mg^{2+} ions occupy HCP sites and hydroxides (OH^-) occupy octahedral sites [56].

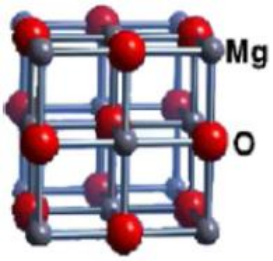

Figure 2.6 Crystallographic structure of FCC magnesium oxide [54], reprinted with permission from the publisher.

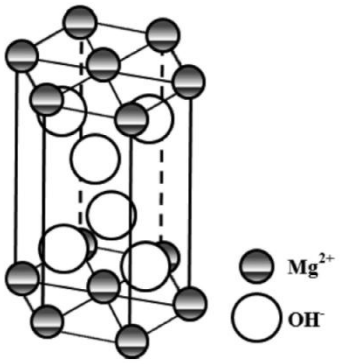

Figure 2.7 Crystallographic structure of HCP magnesium hydroxide where a=b=0.3142 nm and c=0.434 nm [57], reproduced by permission of ECS-The Electrochemical Society.

2.7 Electrochemical Deposition of MgO Coating

Magnesium oxide as a ceramic has typical properties of ceramics such as high refractoriness, high melting temperature, and good corrosion resistance [58], which make it a candidate for high temperature applications. In electrolytic processing of magnesium oxide, first magnesium hydroxide is deposited on the substrate using the electrochemical process and then the magnesium hydroxide is converted to magnesium oxide in a sintering process in the furnace. The morphology and structure of the coating dictates the application.

Electrochemical deposition of magnesium oxide on metallic substrates was reported by Hashaikeh, 2000 [11, 12]. In this research, a three-layer TBC was fabricated. First, NiCoCrAlY in the form of a powder was deposited using electrophoretic deposition. Then magnesium hydroxide was electrolytically deposited as the second layer on the NiCoCrAlY layer and sintered at 850°C. Finally Yttria Stabilized Zirconia (YSZ) powders were also deposited electrophoretically, dried and sintered. It was reported that using lower current densities (less than 5 mA/cm^2) gave a more uniform and crack free magnesium oxide coating [12].

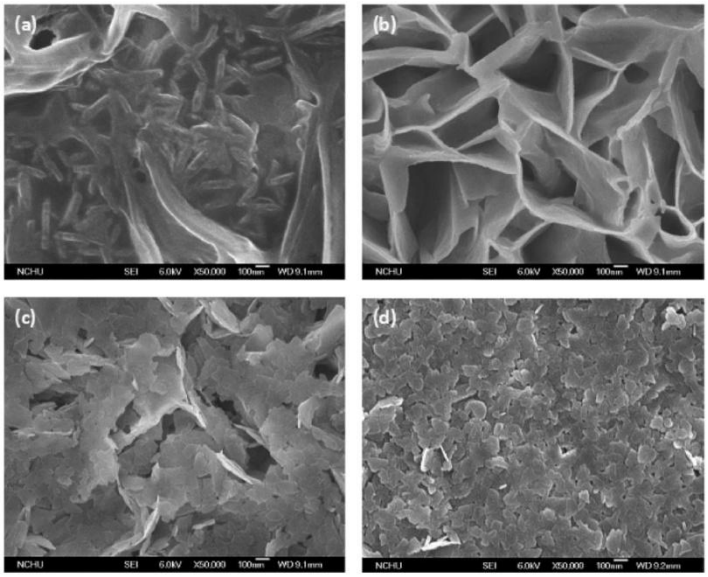

Figure 2.8 Microstructure of magnesium hydroxide deposited for 1800 s at deposition voltage of (a) -0.7 (b) -0.8, (c) -1 and (d) -1.2 V (Ag/AgCl) [57], reproduced with permission of ECS-The Electrochemical Society.

In another comprehensive study on electrolytic processing of magnesium oxide on platinum, the effects of applied voltage on the morphology and structure of the magnesium hydroxide was investigated. It was concluded that with increasing the voltage, the morphology of magnesium hydroxides changes from a lamellar to fine particles [57]. Figure 2.8 shows different morphologies resulting from different voltages. It was also reported that growth happens in preferred orientation of (001) [57]. It was concluded that by increasing voltage, the morphology of the deposited magnesium hydroxide becomes finer. Comparing Figure 2.8(c) and (d) shows that the microstructure has become finer using higher applied voltage [57].

In electrolytic deposition of magnesium hydroxide, the cathode was the substrate material, and the anode was a bar of graphite. The electrolytic solution was a mixture of magnesium nitrate ($Mg(NO_3)_2.6H_2O$) dissolved in distilled water. The following reactions were suggested:

- disassociation of magnesium nitrate in water [11]:

$$Mg(NO_3)_2 \rightarrow Mg^{2+} + 2NO_3^- \quad (2.5)$$

- evolution of hydrogen bubbles at cathodic side [57]:

$$2H^+ + 2e^- \rightarrow H_2 \quad (2.6)$$

- electrolysis reaction of water at the cathodic side [57]:

$$2H_2O + 2e^- \rightarrow H_2 + 2OH^- \quad (2.7)$$

- reduction of oxygen at the cathodic side [57]:

$$O_2 + 2H_2O + 4e^- \rightarrow 4OH^- \quad (2.8)$$

- formation of magnesium hydroxide [57]:

Mg^{2+} ions will be hydrolyzed by produced hydroxides from the reaction (2.7) and (2.8) according to the following reactions ((2.9) and (2.10)) and magnesium hydroxide will be deposited on the cathode.

$$Mg^{+2} + 2OH^- \rightarrow Mg(OH)_2 \quad (2.9)$$

$$Mg^{+2} + 2H_2O + 2e^- \rightarrow Mg(OH)_2 + H_2 \quad (2.10)$$

- calcination reaction [11]:

The deposited $Mg(OH)_2$ in this stage, will be converted to MgO as a result of calcination of magnesium hydroxide at 300 ºC [11]:

$$Mg(OH)_2 \rightarrow MgO + H_2O \quad (2.11)$$

CHAPTER 3

MATERIALS AND METHODS

3.1 Materials

The substrate material was a sheet of SAE 316L stainless steel with the composition given in Table 3.1 and a thickness of 1.5 mm. The sheet was cut in pieces of 25mm×15mm. In order to have exactly the same surface area of deposition, samples were covered with special anti-corrosion tapes (portholes electrochemical sample mask, Gamry), which have a 1cm^2 hole as shown in Figure 3.1(a). This makes it easier to compare samples coated using different deposition parameters. The actual image of the sample covered with these masks is shown in Figure 3.1(b).

Table 3.1 Chemical composition of stainless steel SAE 316L supplied by Parker Steel. International.

Element	Fe	Mn	Ni	Cr	Mo	Si	C
Percentage	Bal	1.85	12.67	18.85	2.3	0.38	0.05

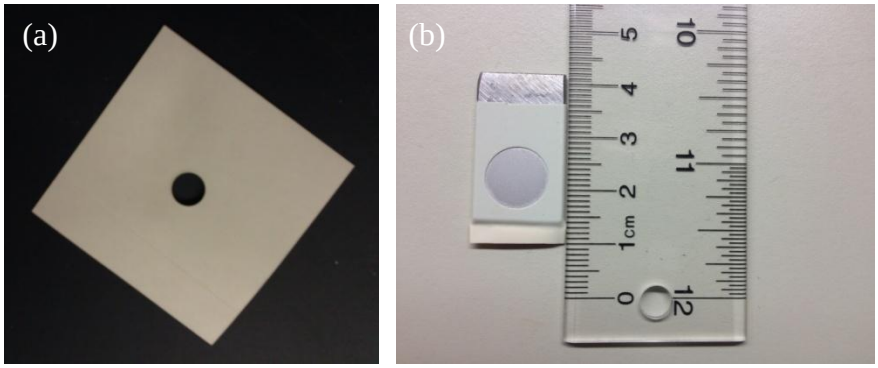

Figure 3.1 (a) Electrochemical sample mask supplied by Gamry, (b) sample covered with the mask.

To make the electrolytic solution, 0.1 M of $Mg(NO_3)_2.6H_2O$ (with purity of 98% from Alfa Aesar Company) was dissolved in distilled water. The prepared solution was poured into a 500 ml beaker. A bar of graphite with dimensions of 30mm×50mm was used as anode.

3.2 Experimental Procedure

Samples were covered with the anti-corrosion mask, weighed using TORBAL AGCN200 digital scale with precision of 0.0001 mg and electropolished in 15% sulfuric acid solution for 4 minutes at a constant current of 0.4 A. This was necessary to remove the chromium oxide layer and activate the surface of the substrate. The specimen was immediately rinsed with distilled water and immersed in the electrolytic bath.

3.2.1 Electrolytic Deposition

A Gamry Series G^{TM}750 potentiostat was used as the power supply and the electropolished sample was the working electrode. The graphite bar was connected to the counter electrode. The potentiostat recorded the variation of current during the deposition. No stirring was used during electrolytic deposition. The sample was removed from the electrolytic bath after deposition and dried in air for 48 hours, weighed, and put into the furnace, MTI Corporation GSL-1500X-50, for the sintering process. Deposition time range was between 5 and 90 minutes and deposition voltages was changed from 1200 mV to 1800 mV. Each point in the optimization curves presented in chapter 4 is an average of three measurements. Voltage and time were used as deposition parameters to optimize the microstructure of the magnesium oxide coating. The weight of the magnesium hydroxide coatings was calculated by subtracting the weight of the sample before deposition from the weight after deposition.

3.2.2 Sintering

Sintering was done in a MTI Corporation GSL-1500X-50 tube furnace under argon gas atmosphere. To make sure that oxygen was removed, a high pressure (20 psi) flow of argon gas passed through the tube furnace for 10 minutes and then the flow pressure was decreased and maintained at a low value (3 psi) during the sintering process. To ensure that the flow was

maintained, the outlet of the gas from the furnace was placed in a beaker full of water. Evolution of bubbles indicated the maintenance of the argon gas flow. Figure 3.2 shows the sintering set-up.

In the sintering step magnesium hydroxide is converted to magnesium oxide at 300°C as a result of a calcination reaction. The calcination reaction starts at 300°C and is completed at 500°C, however higher sintering temperatures is needed to ensure good adherence of the coating to the substrate. Since ceramics has relatively high sintering temperatures, formation of a good bonding layer between the ceramic coating and metallic substrate is less likely at low sintering temperatures. It was reported that sintering of the electrolytically deposited MgO with NiCrAlY interlayer on the substrate of inconel at 1100°C results in a dense MgO layer [12]. There are however limits in increasing the sintering temperature above 1000°C. Sintering at temperatures higher than 1000°C leads to formation of iron oxides which may contribute to cracking of the coating. After various experiments and analysis of the obtained coating at sintering temperatures ranging from 600°C to 1400°C with SEM and XRD, the sintering temperature of 1000°C was chosen and the adopted heating rate was very slow especially between 300°C and 500°C when the calcination reaction starts and finishes. Figure 3.3 shows the heat treatment regime used in the sintering process. It should be mentioned that the anti-corrosion masks were removed from the samples after electrolytic deposition and samples weighed after sintering. Weight of the magnesium oxide coating was weight of the original sample subtracted from the weight of the sample after sintering.

Figure 3.2 Set-up used for sintering experiments.

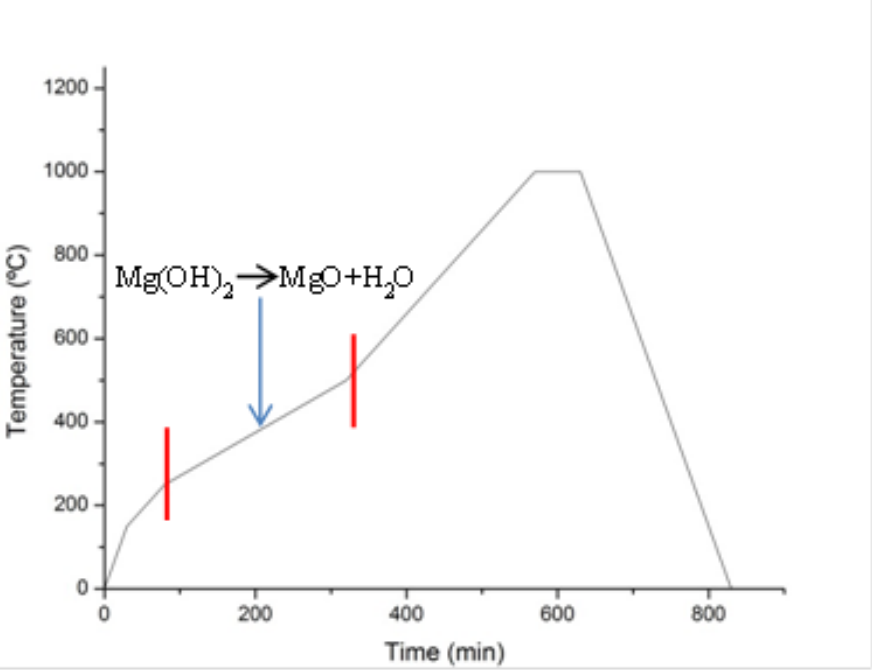

Figure 3.3 Heat treatment regime used for sintering of the coating.

3.3 Characterization

3.3.1 Phase Identification

A Bruker D8 Discover area diffractometer with Cu-K∝ radiation was used for identification of phases of the magnesium hydroxide and magnesium oxide coatings. The voltage and current were set to 40 kV and 40 mA, respectively. Diffraction pattern were collected in steps of 0.04º and three θ-2θ scans were measured and combined to collect the diffraction pattern in the range of 16º-76º.

3.3.2 Texture Measurement

In this project incomplete (100) and (101) pole figures were measured using the scheme shown in table 3.2 and Resmat software was used to calculate the ODF and recalculate (101) pole figures. The IPF of a compact and porous magnesium hydroxide structures is also calculated and discussed in chapter 4. 2θ angle listed in Table 3.2 is the diffraction angle, and ω and Ψ are

sample orientation angles in XRD sample stage, which are marked in Figure 3.4. Table 3.2 shows that the 3 runs were used to collect frames needed for texture analysis at 2θ, ω and Ψ angles.

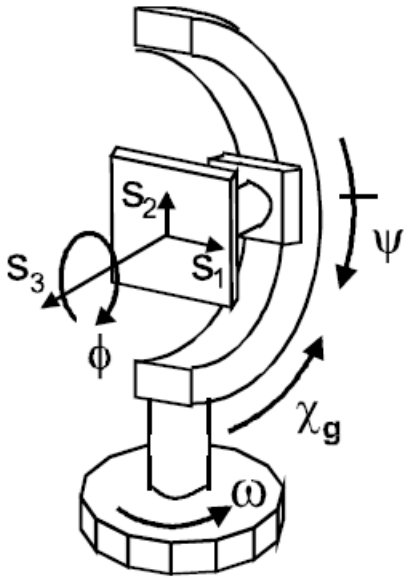

Figure 3.4 Schematic drawing of a sample stage showing sample orientation angles, [59], reprinted with permission from the publisher.

Table 3.2 The scheme used for measuring the texture of magnesium hydroxide coatings.

run	frame	2θ	ω	Ψ	Number of frames	Time (sec)
01	001	28.000	9.100	2.500	36	25.00
02	001	28.000	23.100	31.100	72	25.00
03	001	60.000	31.100	16.100	72	40.00
03	073	60.000	30.400	55.700	72	40.00

3.3.3 Microstructural Analysis

A Hitachi SU6600 SEM equipped with EDS was used for microstructural analysis and Aztec was used as the post-processing software for gathering line and map scans. For taking SEI (secondary electron) and BSI (Back-scattered electron) images and EDS scans, the parameters shown in Table 3.3 are used.

Table 3.3 Parameters used to acquire SEI and BSI images and EDS scans.

	Acceleration voltage (kV)	Emission current (nA)	Working distance (mm)
SEI	2	30000	10
BSI	10	30000	20
EDS	20	30000	10

3.4 Oxidation Tests

Cyclic oxidation method described by Dinesh Gond, et al. [60] was used to evaluate oxidation resistance of the coatings. In this method the samples are heated at certain temperature in a furnace for a certain time, removed from the furnace, weighed and the cycle is repeated until no weight change is detected. Four samples were tested; coated, non-coated, coated covered with corrosive salts and non-coated covered with corrosive salts. Corrosive salt was a paste of Na_2SO_5 and NaCl with the composition given in Table 3.4 to simulate an ash corrosion situation. Samples were oxidized in a Lindberg Blue box furnace. For each test coated and non-coated samples were weighed with the crucible using, placed in the furnace and heated to 900°C and kept at that temperature for an hour, then removed from the furnace and cooled to room temperature for 30 minutes in air. Then the weight was recorded and the specimens were placed in the furnace at 900°C for another hour and this cycle was repeated for 48 hours. Although after some cycles the coatings spalled off to the crucible, the overall weight of oxide was measured.

Table 3.4 Chemical composition of corrosive salts [60].

Element	Na_2SO_5	NaCl
Wt%	75	25

3.5 Corrosion Tests

A Gamry Series G^{TM}750 potentiostat was used for room temperature corrosion tests. Tafel test was done at room temperature using the potentiostat at anodic scan rate of 1 mV/sec, initial voltage of -250 mV vs. E_{oc}, final voltage of 250 mV vs. E_{oc} and the sample period of 1 second. E_{oc} is open circuit potential in equilibrium state. Sample area was 0.382 cm^2. The samples coated with magnesium oxide were covered with the anti-corrosion masks, which had 1cm^2 hole to have exactly same area of testing. This makes it easier and more accurate to compare the results of different samples. In the same way as for the electrolytic deposition, the

sample was connected to the working electrode, but counter electrode was different and wire of platinum was connected to the counter electrode. The distance between cathodes was 2 cm and the solution was 3.5wt% NaCl in distilled water. After connecting the electrodes, the sample and the platinum wire were immersed in the solution for 30 minutes to stabilize the potential of the sample. Then the Tafel test script was selected from the menu of the potentiostat software and the Tafel test started. For calculation of corrosion current, potential and rate, Gamry Echem Analyst software was used. For high temperature corrosion tests, an ash corrosion environment was simulated by applying a thin layer of salt, with the composition given in Table 3.4, onto the samples. The powders were mixed in an ethyl alcohol and a paste of the mixture applied to the coating surface by brush in the amount of 3-5 mg/cm^2 after preheating the samples in the furnace at 250°C for an hour. The specimens were then heated at 250°C for an additional 3 hours. Then, the samples were weighed and the same procedure that was used for cyclic oxidation was repeated.

3.6 Mechanical Tests

Nano-hardness tests were carried out by nano-indentation using a CETR NH-type nano-head from Hysitron Company on the deposited coatings. The non-coated sides of the samples were stuck to a metallic steel stub with crystal bond 509 Amber glue and put under microscope for nano-hardness measurements.

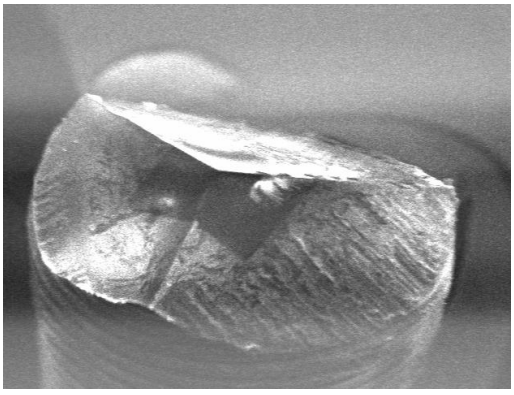

Figure 3.5 Tip of Berkovich indenter, image reproduced with permission from Hysitron, Inc. (Minneapolis, MN) ©Hysitron, Inc.

The hardness was measured at 9 points and the average hardness is reported. Indenter maximum force was 10mN with loading and unloading rate of 0.667 mN/sec and the maximum load was applied for 10 seconds. Rest time was 45 seconds. Indenter was berkovich type. Berkovich is a three-sided pyramidal nano-indenter. Total included angle of the tip of this indenter is 142.3 degree and the half angle is 65.35 degree. Radius of the tip curvature is 150 nm [61]. Figure 3.5 shows the tip of a Berkovich indenter.

CHAPTER 4

RESULTS AND DISCUSSION

4.1 Overview of Chapter 4

In this chapter results and discussion in two separate sections will be presented. As mentioned earlier fabricating magnesium oxide coating consists of two steps: electrodeposition of magnesium hydroxide and a sintering process where magnesium hydroxide is converted to magnesium oxide. To have a uniform magnesium oxide coating, deposition of appropriate magnesium hydroxide in an electrolytic bath is necessary. In this chapter different aspects of electrolytic deposition of magnesium hydroxide will be discussed in detail. Then, the sintering step will be discussed and the results of characterization of the mechanical and corrosion properties of magnesium oxide will be presented.

4.2 Electrolytic Processing of Magnesium Hydroxide

Electrolytic processing of magnesium hydroxide was carried out using the procedure described in chapter 3. Various tests and characterizations of the resulting deposition will be presented.

4.2.1 Identification of Magnesium Hydroxide

Diffraction pattern used for phase identification is shown in Figure 4.1. The first four peaks of the diffraction pattern ((001), (101), (102) and (110) planes are in good agreement with brucite (magnesium hydroxide) pattern [JCP2.2CA:00-007-0239] and this confirms that the coating is magnesium hydroxide.

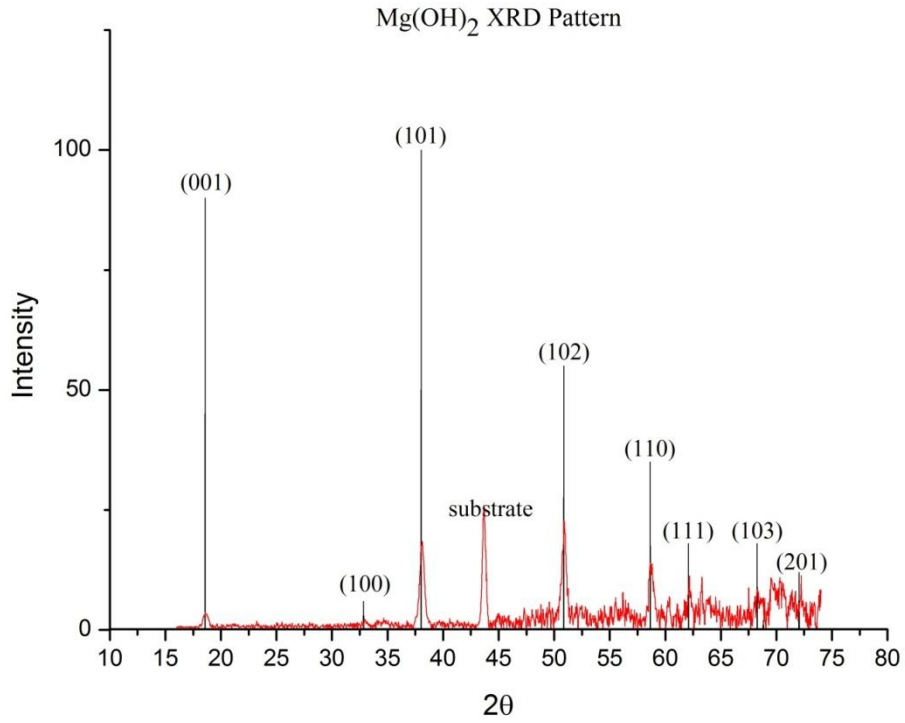

Figure 4.1 X-Ray diffraction pattern of $Mg(OH)_2$ coating deposited on stainless steel substrate at a voltage of 1300 mV.

Since the coating was thin (less than 20 microns), some peaks of the substrate were also detected in the magnesium hydroxide XRD pattern. Relative intensity of peaks in the fabricated coating is different from the standard XRD pattern of magnesium hydroxide, which indicates the presence of texture in the coating. This will be discussed in more detail later.

4.2.2 Optimization of Deposition Parameters

Variables used for optimization of a uniform and crack-free magnesium hydroxide coating were deposition time and voltage. It is necessary to mention that in some electrolytic processing, the current is kept constant instead of the voltage. This was also tested in this project, but after various experiments it was decided to keep the voltage constant because it gives more uniform microstructure in the coating. Using inappropriate deposition voltage gave a non-uniform and porous structure as shown in Figure 4.2. On the one hand, using a low deposition voltage leads to a porous structure. One the other hand, high deposition voltage increases the

evolution of hydrogen bubbles on the substrate and prevents the nucleation and growth of the magnesium hydroxide on the substrate and a non-uniform magnesium hydroxide coating forms. So, using an optimized deposition voltage is necessary to fabricate a uniform coating.

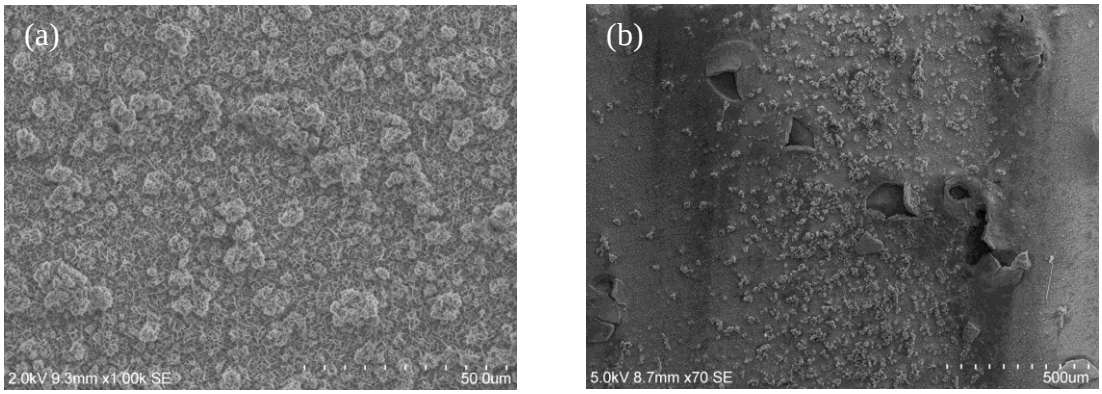

Figure 4.2 SEM image of the magnesium hydroxide coating deposited for 30 minutes at a deposition voltage of: (a) 1000 mV and (b) 1800 mV.

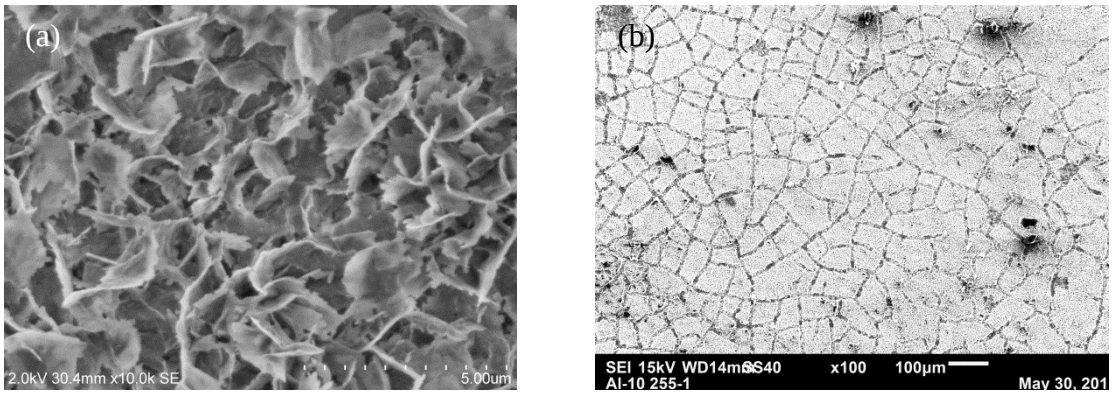

Figure 4.3 SEM image of the magnesium hydroxide coating fabricated at a deposition voltage of 1300 mV and deposition time of: (a) 15 min and (b) 90 min.

Figure 4.3 (a) shows SEM image of the magnesium hydroxide coating deposited at 1300 mV for 15 min which is shorter than the optimized deposition time. The result was a porous structure. Deposition of magnesium hydroxide for a long time (90 minutes) leads to the cracking of the coating after drying, which is shown in figure 4.3 (b). The most uniform and compact structure was observed at a deposition voltage of 1300 mV and a deposition time of 30 min.

4.2.3 Microstructural Analysis of Magnesium Hydroxide

Figure 4.4 shows SEM images of magnesium hydroxide deposied with optimized parameters, at different magnifications. As shown in Figure 4.4(a), the coating is uniform and free of any cracks. Figures 4.4(b) and (c) show high magnifications of the coating, showing that the structure is compact. A higher magnification of the area selected in Figure 4.4(c) is shown in Figure 4.5. The size of the small grains in Figure 4.5 is in the range of 100 nm and this microstructure seems to be the most compact one and showed has the best corrosion and oxidation resistance in this study.

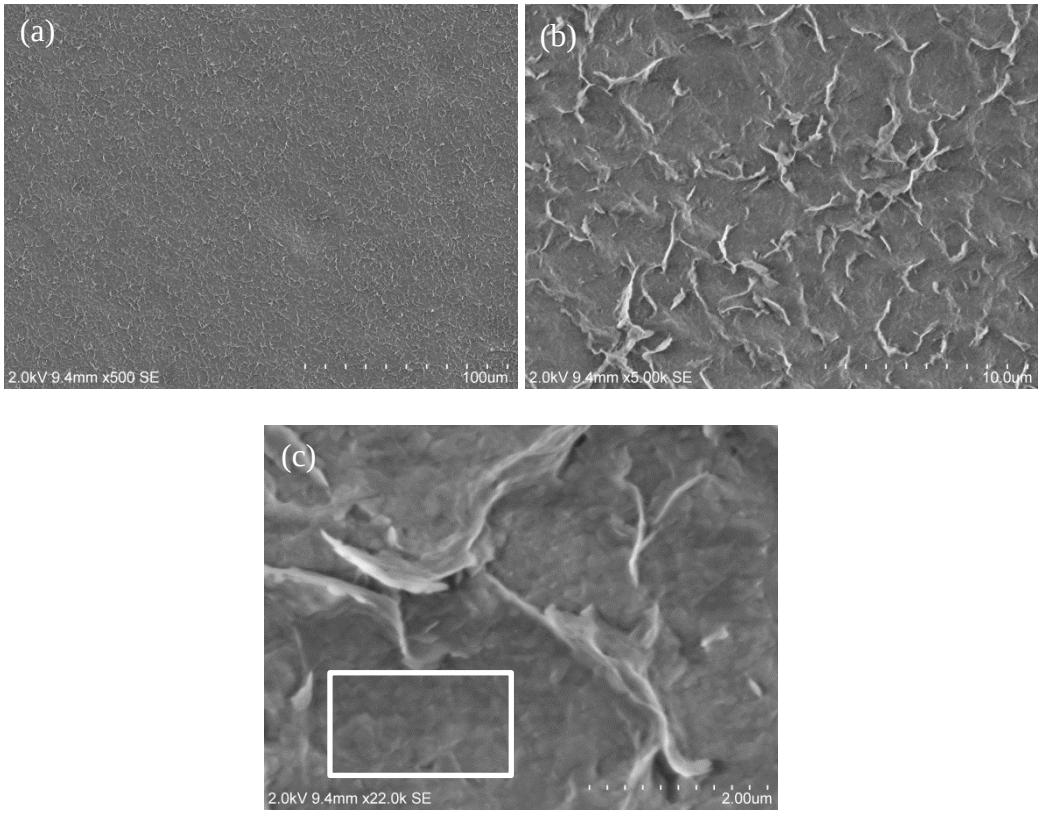

Figure 4.4 SEM image of the coating deposited at a voltage of 1300 mV for 30 minutes: (a) low magnification shows uniform and crack-free coating; (b) and (c) higher magnifications.

Figure 4.6 shows the SEM image of the cross section of the magnesium hydroxide coating processed with optimized parameters, which has compact structure. To make these images, the sample was inclined 70 degrees so that an electron beam could detect the thickness of the coating and image that thickness. The compact structure of the coating is seen in this

figure. The thickness of the coating is about 20 microns. SEM images of the sample that was deposited at a voltage of 1300 mV for 15 minutes is shown in Figure 4.7. It is obvious that the morphology of the coating is porous. One can conclude that this structure forms at the beginning of deposition and then between the porous structure small grains form. The exact mechanism of deposition will be discussed in the section about polarization tests.

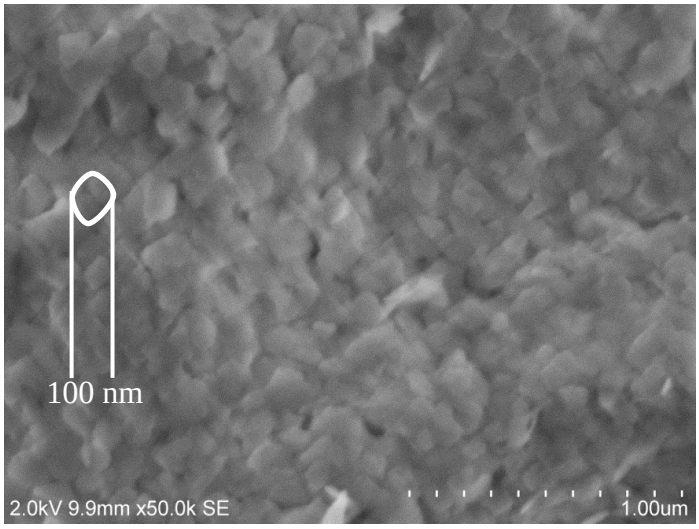

Figure 4.5 SEM image of the coating deposited at a voltage of 1300 mV for 30 minutes, shows the small grains, which are about 100 nanometers in size.

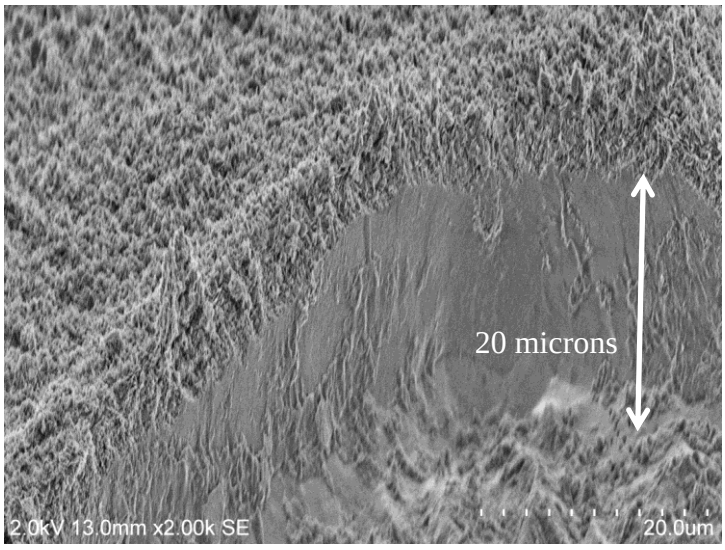

Figure 4.6 SEM image of the cross section of the magnesium hydroxide coating deposited at a voltage of 1300 mV.

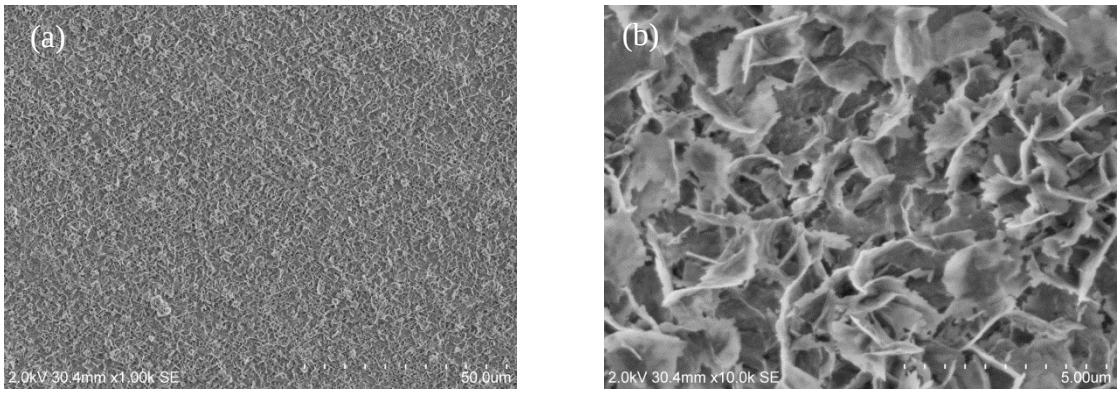

Figure 4.7 SEM image of the coating deposited at a voltage of 1300 mV for 15 minutes, showing porous microstructure at: (a) low and (b) higher magnifications.

4.2.4 Texture Analysis of Magnesium Hydroxide

To have better illustration of the texture of the compact coating, the texture of the porous coating is also measured and compared with the compact coating. Both samples were deposited at 1300 mV, one for 15 minutes and the other for 30 minutes. The results are shown in Figures 4.8 and 4.9. IPF (Inverse Pole Figure) of the direction normal to the film shows a very weak but characteristic texture. The 15 minute sample is characterized by clustering of orientations along the [0001]-[11$\bar{2}$0] lines of the inverse pole figure with maxima at [11$\bar{2}$1].

The 30 minute sample shows crystallites with a spread of orientations along the [0001]-[10$\bar{1}$0] and [0001]-[11$\bar{2}$0] lines of the inverse pole figure. It can therefore, be concluded that there is some change in texture with an increase in deposition time. The difference in texture is further evident from the {101} pole figure, which clearly shows strong intensity at the centre for the 30 minute sample compared to the 15 minute sample. This clearly indicates that the magnesium hydroxide grains are oriented with the {101} plane perpendicular to the growth direction and have compact structures as evident from the SEM images. In the hexagonal system, (0001) is a basal planes, (10$\bar{1}$0) is a prismatic plane and (10$\bar{1}$1), (10$\bar{1}$2) are pyramidal planes. In cubic system, the indices of the direction of the normal of a plane are same as the indices of the plane, but in hexagonal system it is different and should be calculated with other methods.

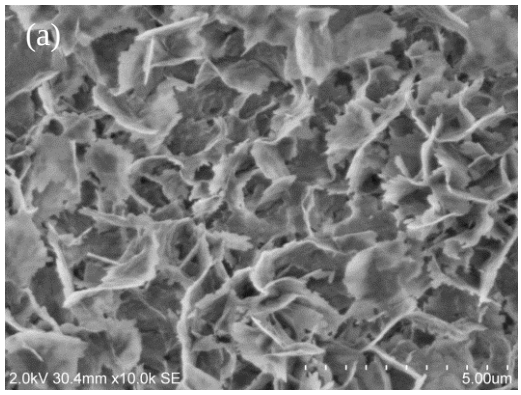

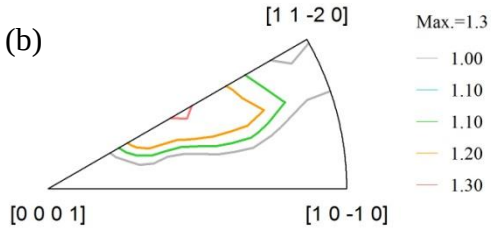

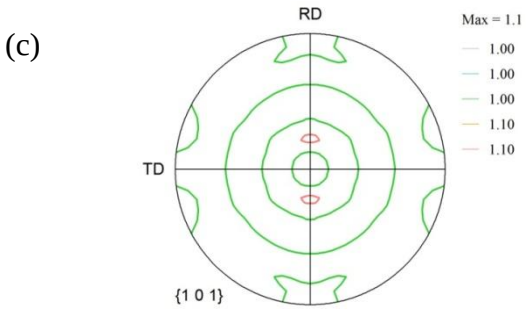

Figure 4.8 Texture of magnesium hydroxide coating deposited at a voltage of 1300 mV for 15 minutes: (a) SEM image, (b) IPF and (c) {101} PF

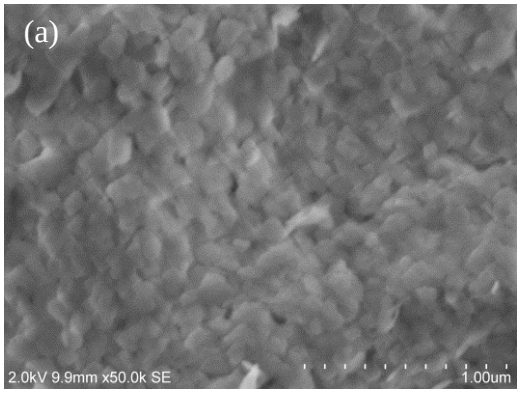

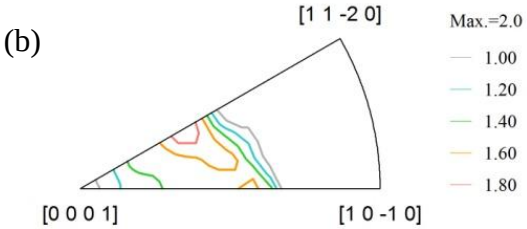

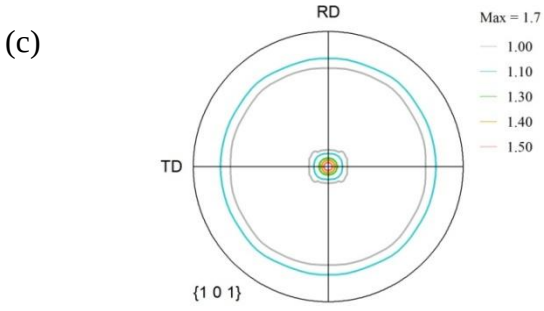

Figure 4.9 Texture of magnesium hydroxide coating deposited at a voltage of 1300 mV for 30 minutes: (a) SEM image, (b) IPF and (c) {101} PF.

4.2.5 Cathodic Polarization and Potentiostatic Tests

The cathodic Polarization curve of SAE 316L stainless steel in a 0.1 M magnesium nitrate solution is shown in Figure 4.10. For deposition of magnesium hydroxide on the substrate, hydroxide ions are needed. Hydroxides are generated mainly from reduction of water (eq. (2-7)) and reduction of oxygen (eq. (2-8)), which is also indicated in Figure 4.10. This is comprehensively discussed by Ching Fei Li [57], who concluded that each of the three sections on the polarization curve corresponds to the reactions indicated in Figure 4.10.

Production of hydroxide from reduction of oxygen requires an oxygen supply, but the amount of oxygen in solution is limited. So, at voltages lower than -1150 mV, the amount of hydroxide formed is limited by the availability of oxygen. As a result the rate of production of hydroxide is low and only a few nuclei will deposit and grow to form a porous structure. On the other hand, at voltages higher than -1150 mV, the reaction of reduction of water is dominant and in such cases there is no limit to the rate of production of hydroxide and this result into a fine microstructure.

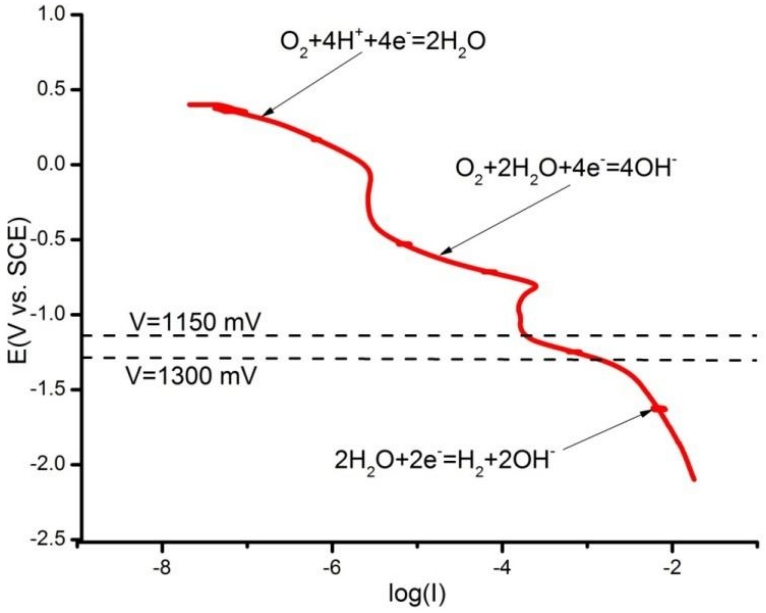

Figure 4.10 Cathodic polarization of SAE 316L stainless steel in a 0.1 M magnesium nitrite solution.

4.2.6 Mechanism of Deposition

At the beginning of deposition, the reduction of oxygen reaction is dominant which leads to a porous structure until oxygen is consumed. Then the reduction of water reaction produces more hydroxides and a finer structure of the deposit will be formed. From a thermodynamic point of view, after formation of a porous structure the concentration of hydroxides, and consequently pH, increases locally between the pores of the structure which results in a higher rate of production of magnesium hydroxide.

Figure 4.11 shows the changes of current versus time at different voltages. As expected, the current suddenly increases, then decreases sharply and finally becomes almost constant. This trend is true for almost all deposition voltages other than 1300 mV where after a while the current increases. This corresponds to high local concentration of hydroxides within porous structures. If (2.7) and (2.9) are added, the overall reaction that produces $Mg(OH)_2$ is:

$$Mg^{2+}+2H_2O+2e^-=Mg(OH)_2+H_2 \quad (4.1)$$

As is obvious from eq. (4.1) increasing current means a higher deposition rate of magnesium hydroxide and as a result more hydrogen bubbles will be released. In fact a higher number of hydrogen bubbles were observed during all experiments as time progressed.

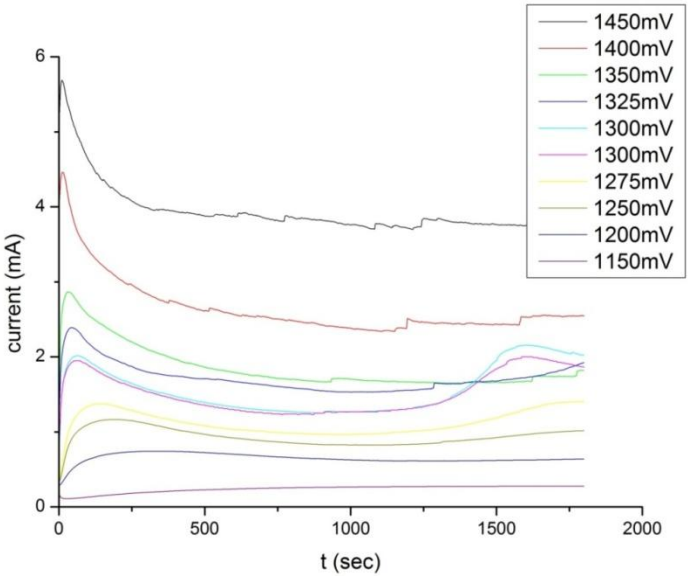

Figure 4.11 Potentiostatic curves of electrodeposition of magnesium hydroxide on SAE 316L stainless steel at different voltages.

4.2.7 Effect of Applied Voltage on Morphology of Magnesium Hydroxide

Not only deposition time, but also applied voltage can greatly change the morphology of the magnesium hydroxide coating. As discussed earlier the two major reactions that produce hydroxides determine the morphology of the coating and these reactions takes place at different voltages. So if the experiments are done at single voltage, keeping the voltage constant is really important. In early experiments, where voltage was manually controlled, the results were not as good as in the later potentiostat controlled experiments in terms of uniformity and reproducibility of the coating.

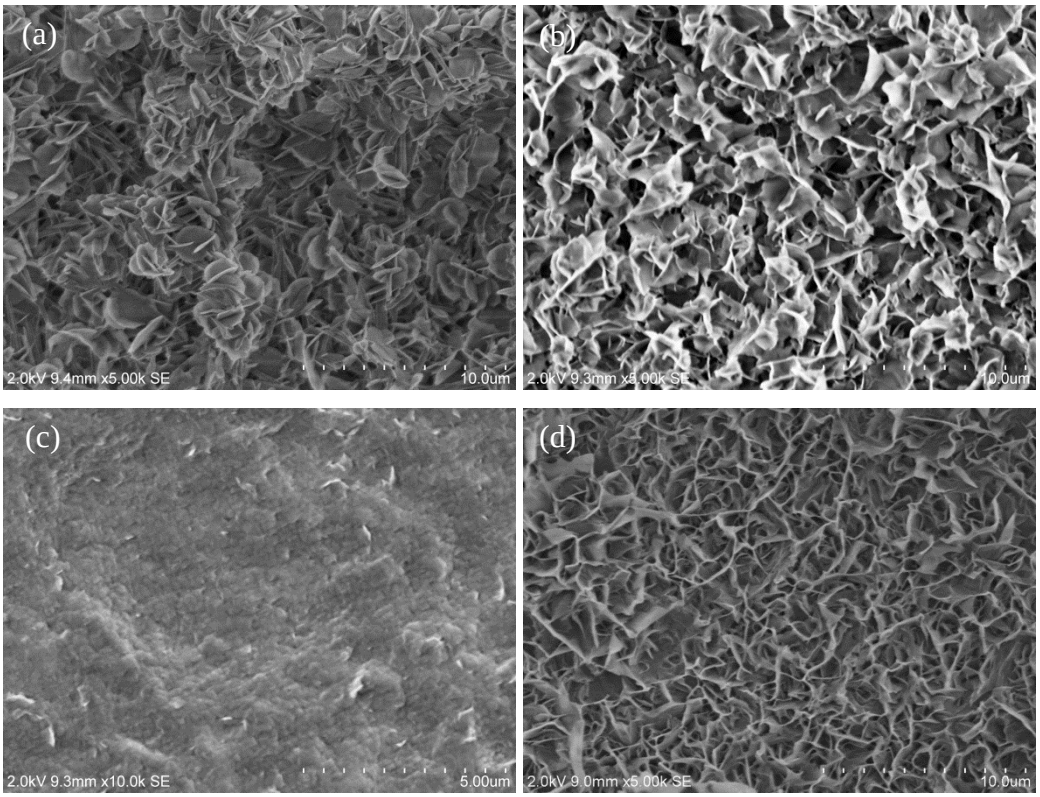

Figure 4.12 Effect of voltage on morphology of the coatings fabricated at deposition time of 30 min and voltages of: (a) 1200 mV, (b)1250 mV and (c)1300 mV and d) deposition time of 15 min and voltage of 1300mV.

Figure 4.12 shows the SEM image of different magnesium hydroxide morphologies deposited with different deposition times and applied voltages. Figures 4.12(a), (b) and (c) are

the samples deposited for 30 minutes at constant voltages of 1200 mV, 1250 mV and 1300 mV respectively. Figure 4.12(c) shows small grains, which indicate it has the most compact microstructure. In fact the rate of production of hydroxides dictates the morphology of the fabricated coating. This rate is not only determined by the type of reaction (i.e. reduction of water or oxygen), but also by the amplitude of voltage. For example in both Figures 4.12(b) and (c), reduction of water reaction produces hydroxides, but the rate of hydroxide production is higher at 1300 mV than at 1250 mV and this results in a finer microstructure with small grains. The effect of deposition time on morphology can be observed by comparing Figures 4.12(c) and (d) as it was discussed earlier.

4.3 Properties of Magnesium Oxide Coating

Different parameters affect the quality of the magnesium oxide coating during the sintering step. These parameters will be discussed and structure and corrosion test results will be analyzed in this section.

4.3.1 Optimization of Sintering Parameters

Sintering at high temperatures leads to the oxidation of substrate. Oxides growing on the substrate may contribute to cracking or removal of the coating. Figure 4.13 clearly illustrates this problem. To avoid oxidation, the sintering process was done in an argon gas atmosphere, which prevented oxidation. Although a calcination reaction can be completed at temperatures lower than 500°C, the adherence of magnesium oxide to the coating is not good enough at low sintering temperatures. The higher the sintering temperature, the better the adherence of the coating to the substrate; however avoiding the oxidation of the substrate is still important. The best scenario is to have spinel of magnesium and iron or chromium as an interlayer between the magnesium oxide coating and the stainless steel substrate. Such an interlayer can significantly improve the adherence of the coating to the substrate. However there are limits to increasing the temperature, including substrate melting and a high rate of oxidation at high temperatures. Microstructural analysis showed that the maximum sintering temperature without growing of oxides of the substrate was 1000°C under argon gas atmosphere.

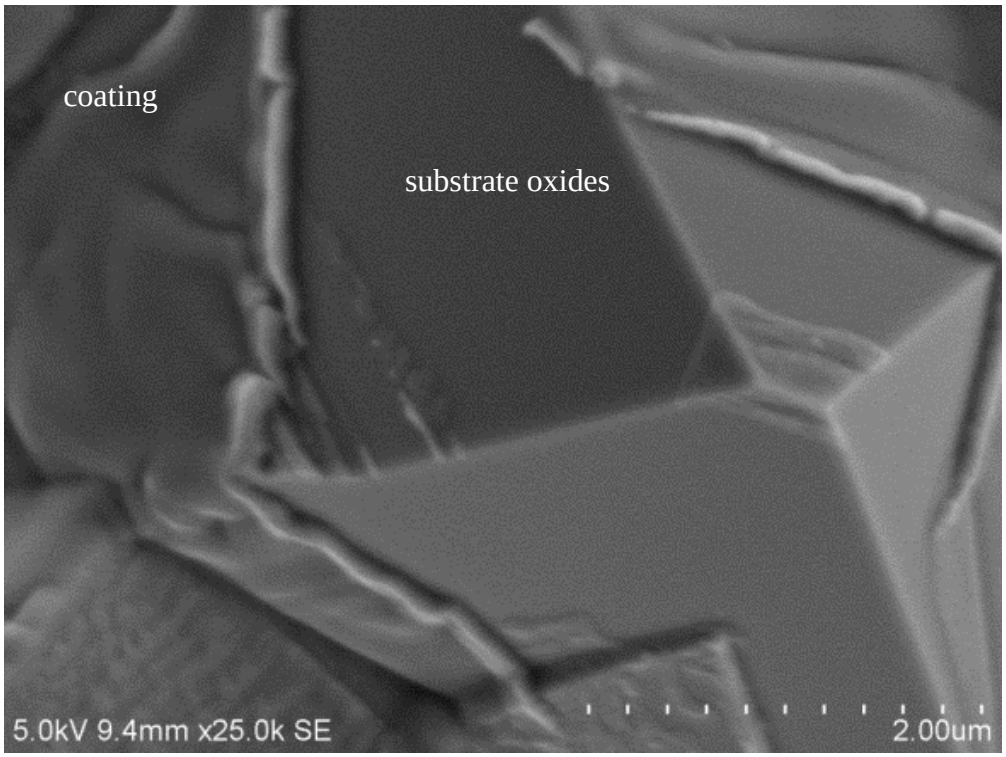

Figure 4.13 SEM image shows how the oxides formation on the substrate removes the coating at sintering temperature of 1200°C and oxidizing atmosphere.

4.3.2 Identification of Magnesium Oxide

The structure of the magnesium oxide coating was analyzed by XRD. As shown in Figure 4.14, the first four peaks of the diffraction pattern ((200), (220), (111) and (311) are in good agreement with magnesium oxide pattern. Since the thickness of the coating is about 10 microns, peaks from the substrate are also present in the XRD pattern.

The relative intensity of peaks in this magnesium oxide XRD pattern is different from the standard magnesium oxide XRD pattern [JCP2.2CA:03-065-0476], which is a sign of texture in the coating. This XRD is taken from the coating fabricated using optimized parameters (i.e. deposition time of 30 minutes and applied voltage of 1300 mV).

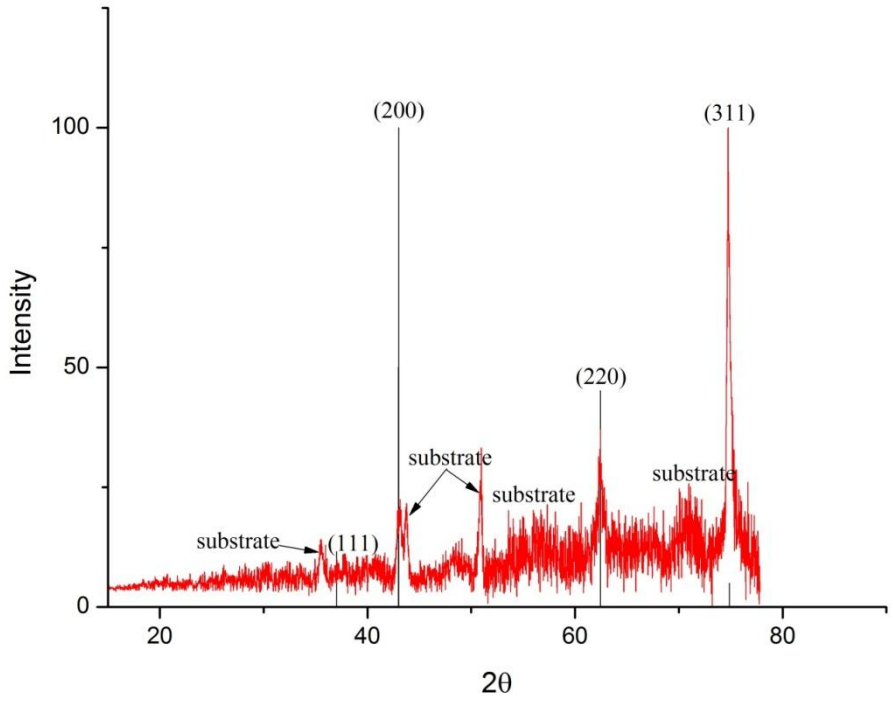

Figure 4.14 X-Ray diffraction pattern for magnesium oxide coating deposited on stainless steel substrate at a voltage of 1300 mV and sintered at 1000°C.

4.3.3 Microstructural Analysis of Magnesium Oxide

Microstructure of MgO coating is dictated by the microstructure of magnesium hydroxide coating. SEM images of the sample sintered at 1000°C are shown in Figure 4.15, which shows that the microstructure of the coating after sintering is the same as the microstructure of the sample before sintering (Figure 4.6) and the structure is compact, which is desirable for corrosion and oxidation resistance applications. A back-scattered image of the cross section of the same coating is shown in Figure 4.16. The thickness of the coating is about 8-10 microns.

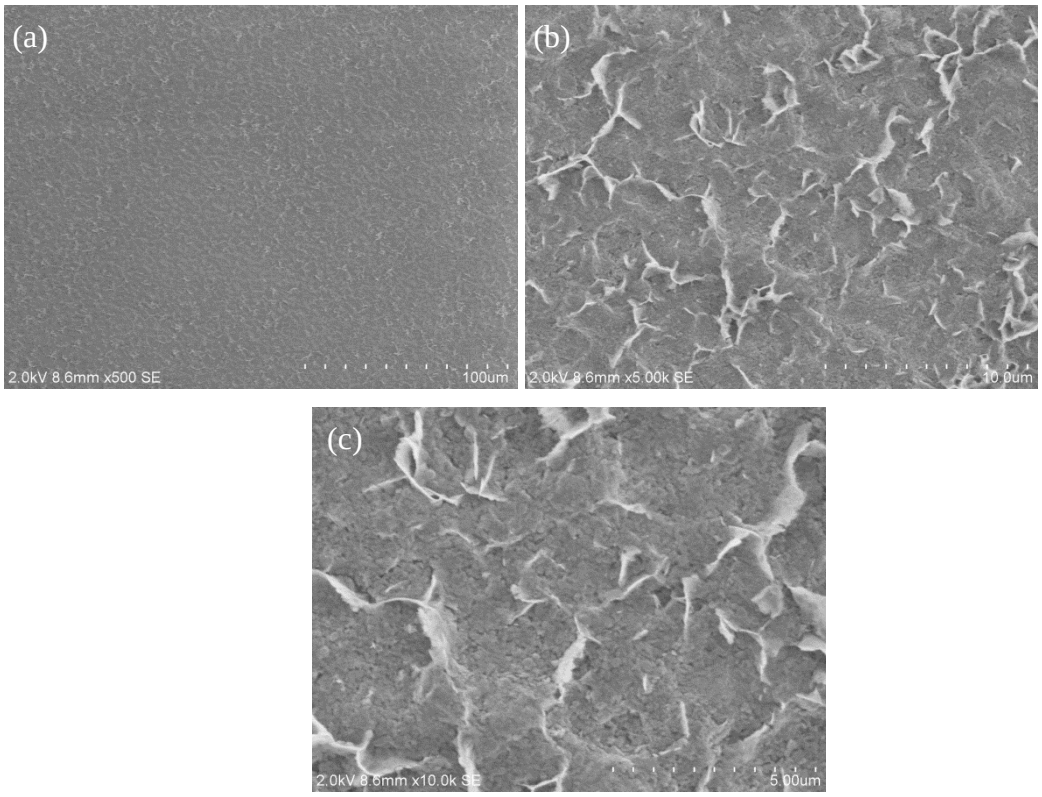

Figure 4.15 SEM image of the coating deposited at a voltage of 1300 mV for 30 minutes and sintered at 1000°C: (a) low magnification shows uniform and crack-free coating, (b and (c) higher magnifications.

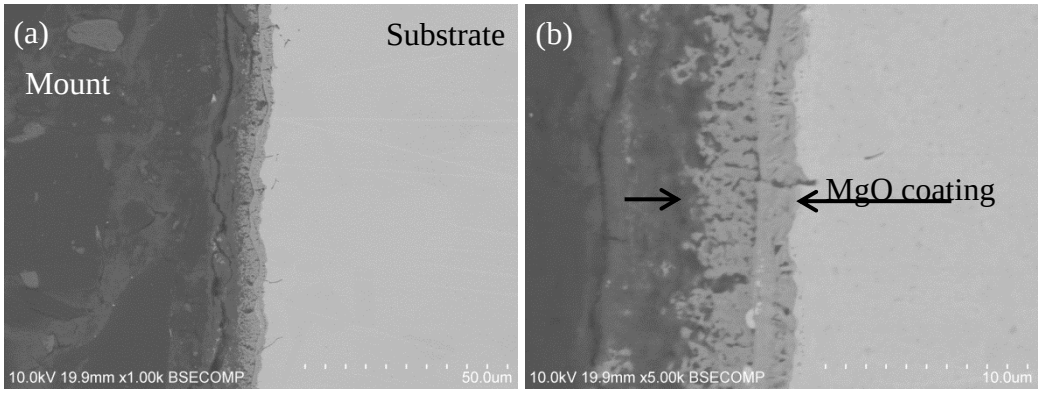

Figure 4.16 Back-scattered images of cross section of the coating sintered at 1000°C: (a) low magnification and (b) higher magnification.

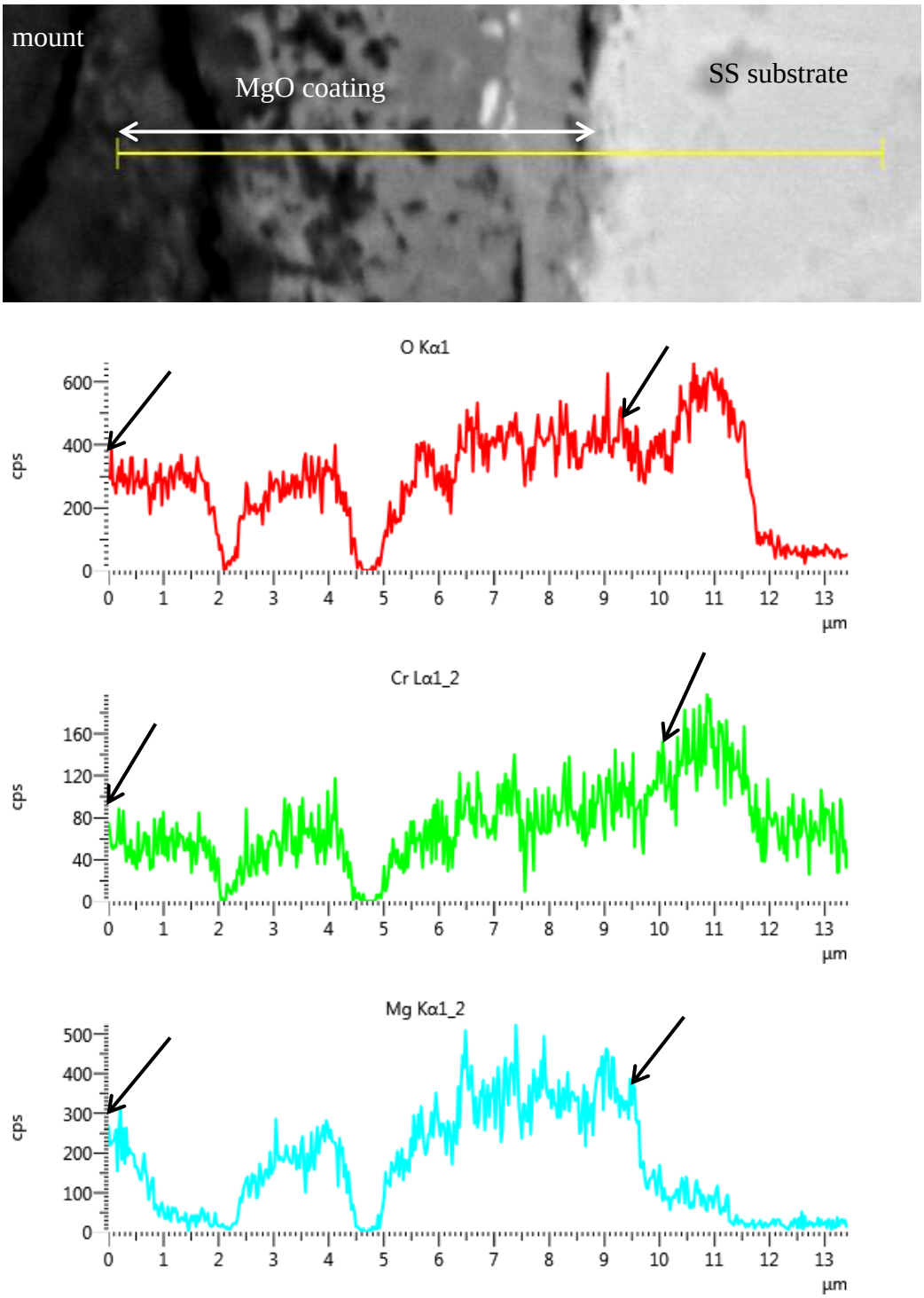

Figure 4.17 Line-scan of O, Cr and Mg presence along the cross section of the coating. The arrows showing the thickness of the MgO coating.

Figure 4.17 shows a line scan of three elements including oxygen, chromium and magnesium and Figure 4.18 shows a map of iron, oxygen and magnesium at the cross section. The line scan of iron, magnesium and oxygen confirms that the coating is magnesium oxide. The thickness of magnesium oxide coating is marked on Figure 4.17 with arrows. Because of the spallation of coating, the intensity of line scans is zero at certain points (note 2 and 5 micron points). The line scan of chromium shows that the content of this element decreases as distance from the substrate increases. It shows that diffusion of the substrate elements such as chromium and iron take place during sintering. This process would possibly improve the adherence of the coating to the substrate by creating an interlayer such as iron and magnesium compounds.

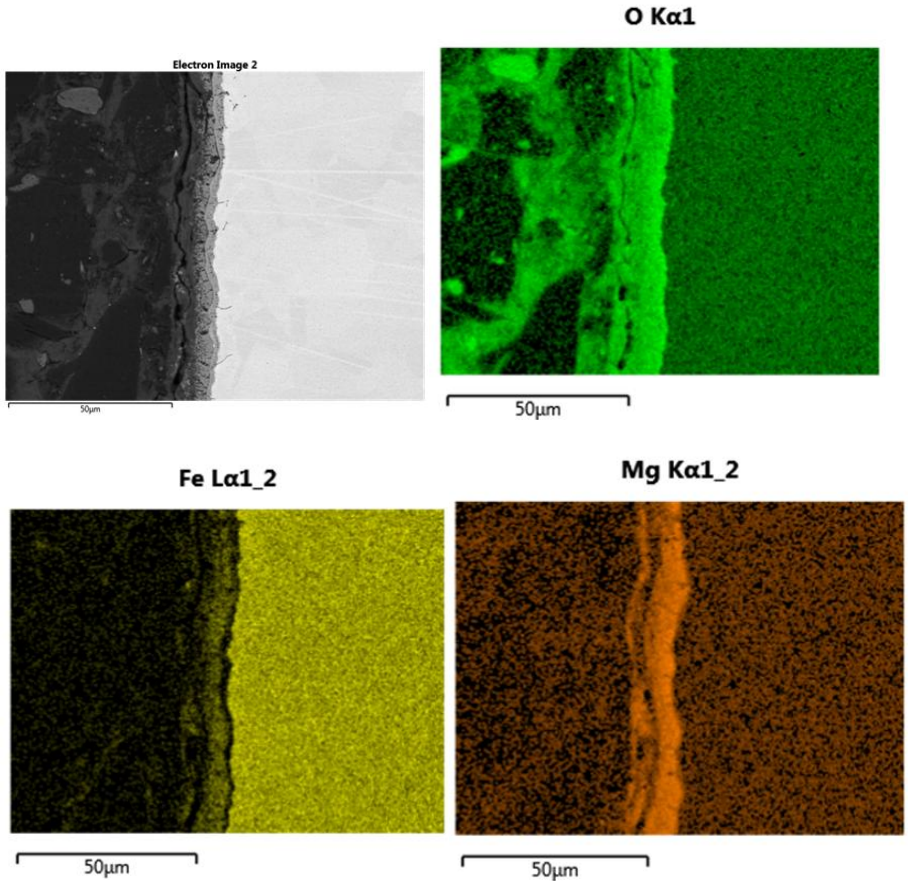

Figure 4.18 Distribution of O, Fe and Mg at the cross section of the coating.

Formation of magnesium, iron and oxygen compounds between the coating and substrate is more likely at higher sintering temperatures. But high sintering temperatures increase the possibility of oxidation. Although sintering was done in an inert gas atmosphere, the argon gas is not very pure and avoiding oxidation at high temperatures is not always possible.

4.3.4 Effect of MgO Coating on the Corrosion and Oxidation Resistance of SAE 316L Stainless Steel

Results of the corrosion and oxidation tests are shown in Figure 4.19. It can be seen that in all cases weight gain increased sharply in the first few hours and then remained virtually unchanged with increasing exposure time. At first few hours of the oxidation or corrosion test, the fresh substrate or coating was exposed to the corrosive environment and was heavily corroded. As the experiment progressed, the corrosion products remained on the surface of the specimens and protect them from further corrosion. So corrosion products protect the substrate from further corrosion. As a result, after sharp increase at the first few hours, the weight gain remained unchanged. Figure 4.19 shows that the oxidation resistance of the coated sample was slightly better than the uncoated sample. The oxidation of uncoated SAE 316L stainless steel at 900°C and after 48 hours of cyclic oxidation was 1.7 mg/cm^2; while that of the coated sample was less than 1 mg/cm^2, which is better than for uncoated sample. The magnesium oxide coating improves significantly the ash corrosion resistance. This is clearly illustrated in Figure 4.19, where the weight gain of the non-coated sample is much higher than on the coated sample. After 48 hours of cyclic oxidation testing, the coated sample gain is less than 6 mg/cm^2, while the non-coated sample has gained more than 20 mg/cm^2, which means that the corrosion resistance increases more than three fold in ash-corrosive environment. This shows that the magnesium oxide coating acts as a barrier for salts, which simulated ash corrosion. Notice that at 900° C, both salts (NaCl and Na_2SO_5) are liquids that can severely attack the surface of the metal.

Figure 4.20 shows SEM images of the coating after oxidation tests. Part of the coating is covered with iron oxides and part with magnesium oxide. This is confirmed by the map scan of magnesium and iron, which is shown in Figures 4.21. The high intensity of magnesium in the magnesium map is related to the magnesium oxide coating. The high intensity of iron in the iron map shows the growth of iron oxide because of cyclic oxidation testing. Note that heating the

sample for 48 hours at 900°C while the sample has undergone heavy thermal shocks (i.e. removing sample from furnace at 900°C after each cycle) created severe testing condition.

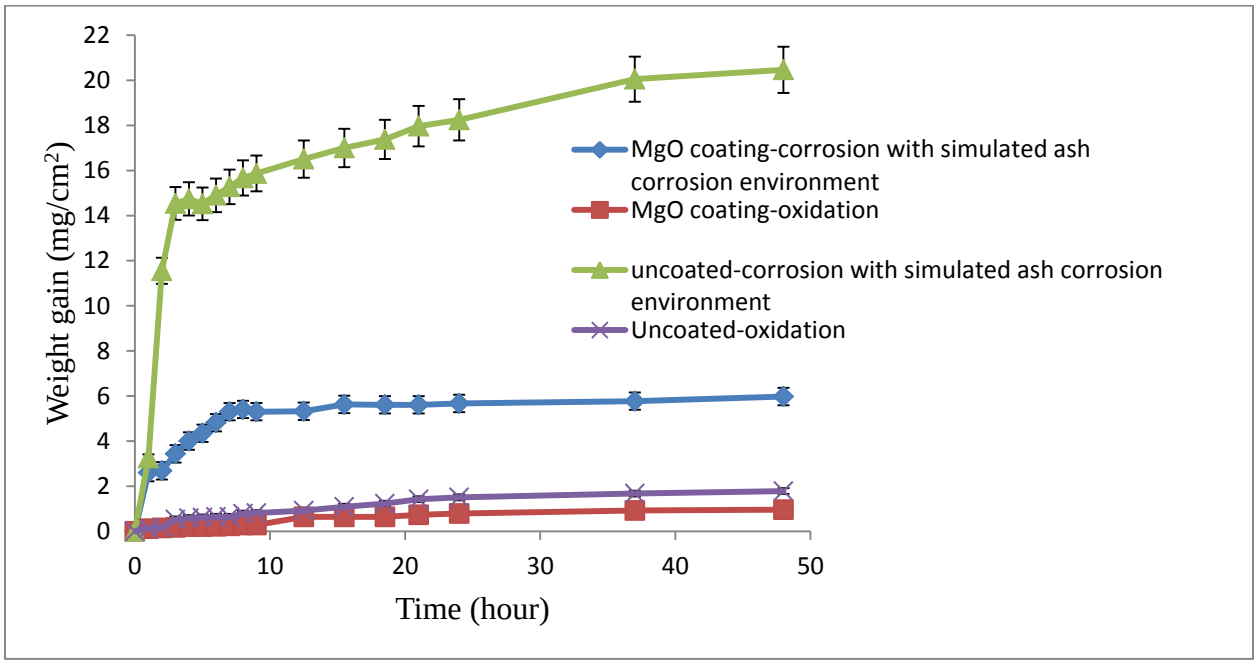

Figure 4.19 Weight gain versus oxidation time for coated and non-coated sample in corrosive and non-corrosive environment oxidized at 900°C.

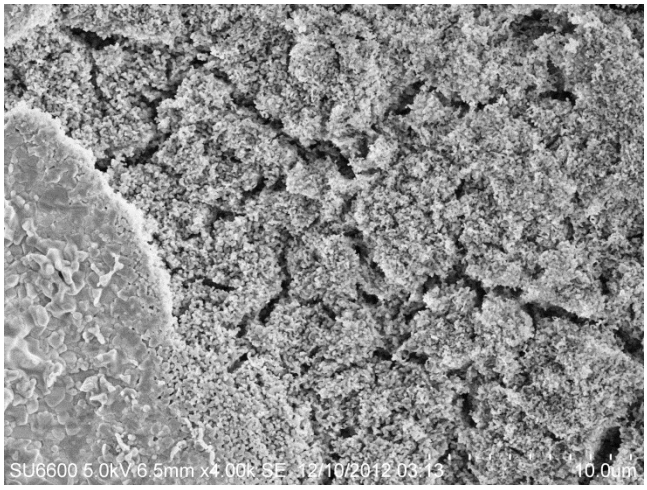

Figure 4.20 SEM image of the sample after 48 hours of cyclic oxidation testing at 900°C.

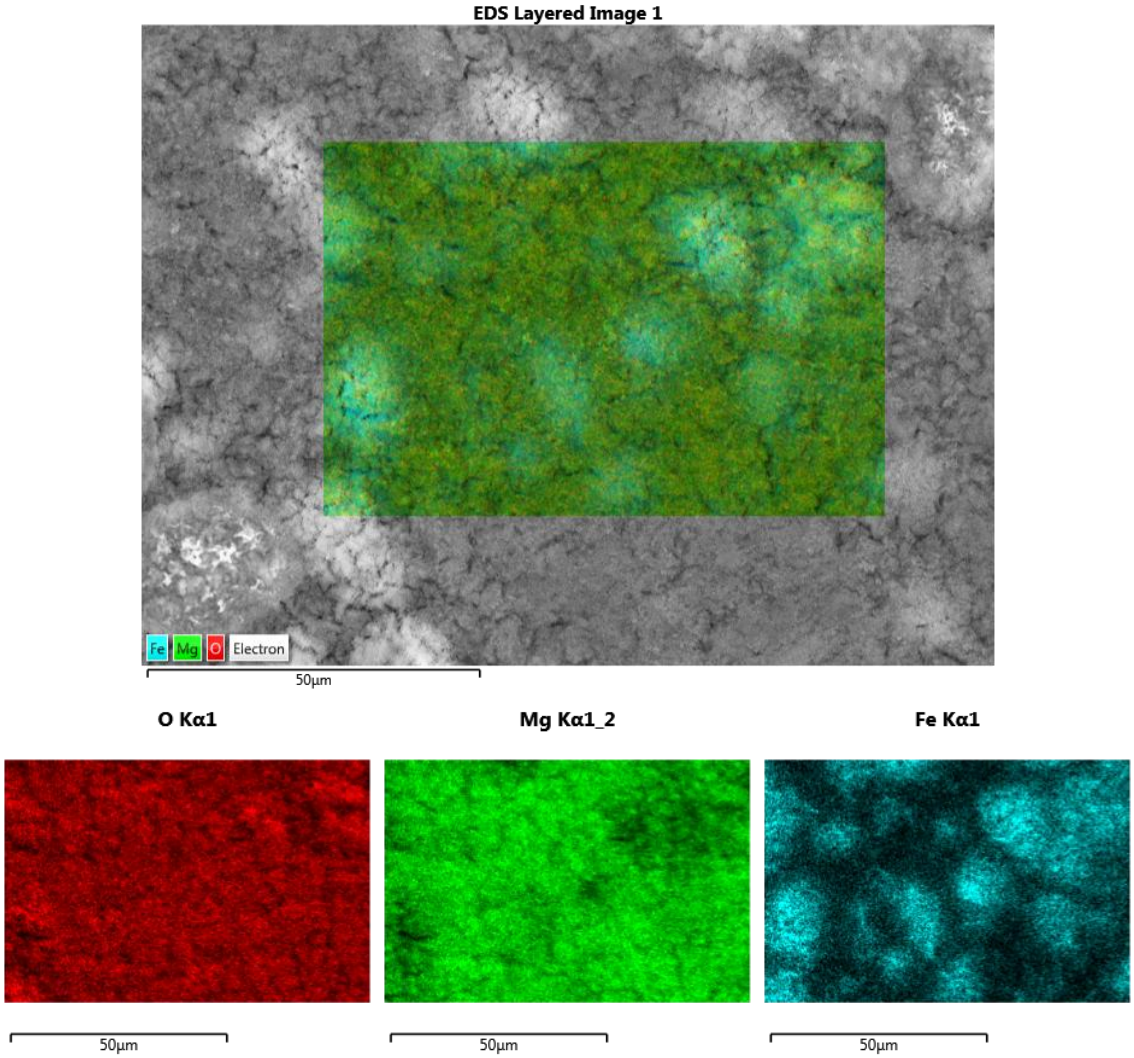

Figure 4.21 Map scan of O, Mg and Fe from the coating of the sample after 48 hours of cyclic oxidation testing at 900^{o}C.

Results of the Tafel test at room temperature are presented in Table 4.1 and Figure 4.22. Comparison of the corrosion rate of the coated and non-coated samples shows that after coating the sample, corrosion resistance increases about eleven fold. Comparing corrosion potentials of the coated and uncoated samples also shows that the coated sample is nobler than the non-coated sample. The corrosion potential of the coated sample is 3 times higher than the non-coated sample.

Table 4.1 Corrosion properties of coated and uncoated samples.

Element	coated	Uncoated
b_a (V/decade)	383.6×10^{-3}	136.0×10^{-3}
b_c (V/decade)	94.70×10^{-3}	149.1×10^{-3}
i corr(nA)	4.8000	53.60
E corr (mV)	-90.40	-263.0
E_{oc} (mV)	-4.071	-249.5
Corrosion rate (mpy)	5.739×10^{-3}	63.98×10^{-3}

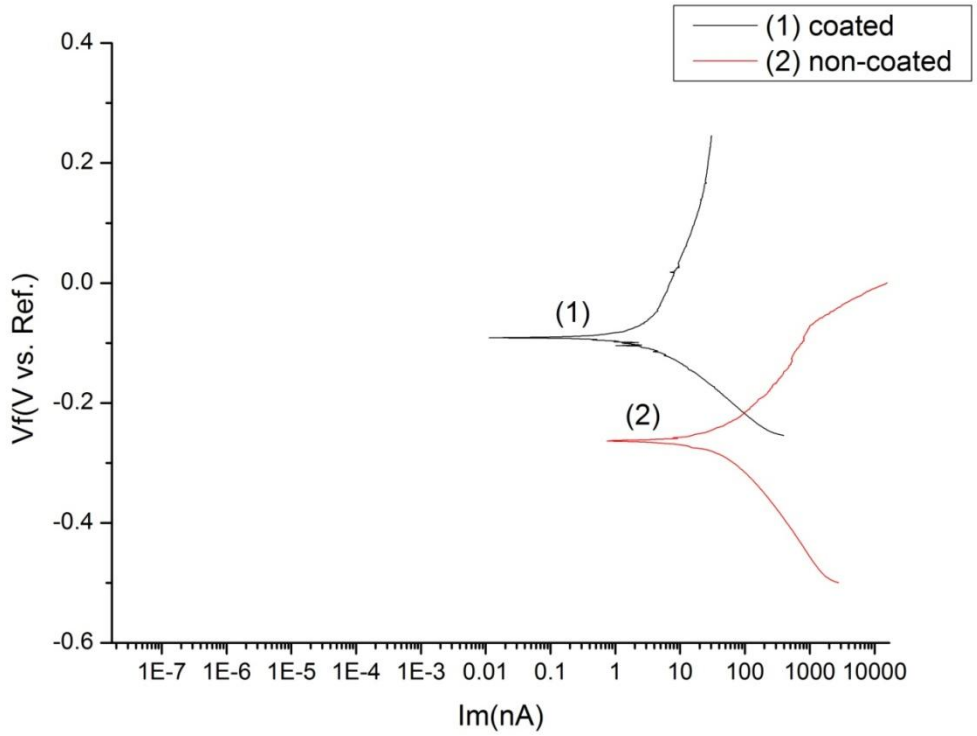

Figure 4.22 Tafel plots of coated and non-coated samples.

4.3.5 Nano-hardness Results

To investigate the mechanical properties of the coating, a nano-hardness test with the method described in chapter 3 was carried out. The measured hardness was 428±32 HV. The maximum hardness of SAE 316L stainless steel is 217 HB [62] or 230 HV. This shows the hardness of the MgO coating is about 86 percent higher than the hardness of SAE 316L stainless steel.

CHAPTER 5

CONCLUSIONS AND FUTURE WORKS

5.1 Conclusions

1. A compact coating of magnesium oxide was electrolytically deposited on SAE 316L stainless steel substrate using the following parameters:
   (i) Deposition voltage of 1300 mV.
   (ii) Deposition time of 30 minutes.
   (iii) 1 hour sintering at 1000^{o}C in argon atmosphere.
2. It was shown that deposition voltage and time changed the morphology of the deposited coatings substantially. By controlling these parameters the desirable morphologies can be obtained.
3. Magnesium oxide coating improved the room temperature corrosion resistance of SAE 316L stainless steel substrate in 3.5% NaCl in water solution by a factor of 11. It also improved its high temperature corrosion resistance in simulated ash corrosion environment by a factor of 3.
4. The measured hardness of magnesium oxide coating was about 86% more than the hardness of SAE 316L stainless steel.

5.2 Future Works

Some topics that can be still investigated regarding the fabrication of magnesium oxide coating are listed below:

1. Evaluation of the adherence of the coating with a scratch test.
2. Introduction of an interlayer to increase the adherence of the coating to the substrate.
3. Evaluate possible method for reduction of oxidation of the substrate.

REFERENCES

[1] Suzuki, I., 1989. Corrosion-resistant coatings technology, Marcel Dekker, Inc.

[2] Hocking, M.G., Vasantasree, V., 1989. Metallic and ceramic coatings: production, high temperature properties & applications, Longman Scientific & Technical.

[3] Pechman, A., 1954. Ceramics for high-temperature applications: A survey of materials used as coatings for, or in combination with, metals, aircraft engineering and aerospace technology, Vol. 26, issue 5, pp. 157 – 160.

[4] Xiong, H-P., Kawasaki, A., Kang, Y.S, Watanabe, R., 2005. Experimental study on heat insulation performance of functionally graded metal/ceramic coatings and their fracture behavior at high surface temperatures, Surface and Coatings Technology, Vol. 194, Issues 2–3, pp 203–214.

[5] Morksa, M.F., Colea, I., Kobayashib, A., 2013. Plasma forming multilayer ceramics for ultra-high temperature application, Vacuum, Vol. 88, pp 134–138.

[6] Bach, F.W., Laarmann, A., Wenz, T., 2006. Modern surface technology, WILEY-VCH Verlag GmbH & Co. KGaA, Weinheim, pp 51- 220.

[7] Boccaccini, A.R., Zhitomirsky, I., 2002. Application of electrophoretic and electrolytic deposition techniques in ceramics processing, Current Opinion in Solid State and Materials Science, Vol 6, Issue 3, pp. 251–260.

[8] Zhitomirsky, I., Petric, A., 1999. Electrolytic and electrophoretic deposition of CeO films, Materials Letters,Vol. 40, No. 6, pp. 263–268(6).

[9] Zhitomirsky, I., Petric, A., 2002. Cathodic electrodeposition of ceramic coatings for oxidation protection of materials at elevated temperatures, Canadian Metallurgical Quarterly, Vol 41, No 4, pp. 497-506.

[10] Zhitomirsky, I., Petric, A., 2001. Electrolytic deposition of ZrO –YO films, Materials Letters, Vol 50, No. 4, pp. 189–193(5).

[11] Hashaikeh, R., Szpunar, J.A., 2009. Electrolytic processing of MgO coatings, Journal of Physics, Conference Series 165 (2009) 01200.

[12] Hashaikeh, R., 2000. Fabrication of thermal barrier coating using electrochemical methods, Master's thesis, Department of Mining and Metallurgical Engineering, Mc Gill University.

[13] Lei, T., Ouyang, C., Tang, W., Li, L-F., Zhou, L-S., 2010. Preparation of MgO coatings on magnesium alloys for corrosion protection, Surface & Coatings Technology, Vol 204, Issue 23, pp. 3798–3803.

[14] Aries, L., 1994. Preparation of electrolytic ceramic films on stainless steel conversion coatings, Journal of Applied Electrochemistry, Vol 24, No 6, pp. 554-558.

[15] Aries, L., Alberich, L., Roy, J., Sotoul, J., 1996. Conversion coating on stainless steel as a support for electrochemically induced alumina deposit, Electrochimica Acta, Vol 41, Issue 18, pp. 2799-2803.

[16] El Hajjaji, S., El Alaoui, M., Simon, Patrice, Guenbour, A., Ben Bachir, A., Puech-Costes, E., Maurette, M.T., Aries, L., 2005. Preparation and characterization of electrolytic alumina deposit on austenitic stainless steel, Science and Technology of Advanced Materials, Vol 6, Issue 5, pp. 519-524.

[17] Boccaccinia, A.R., Zhitomirsky, I., 2002. Application of electrophoretic and electrolytic deposition techniques in ceramics processing, Current Opinion in Solid State and Materials Science, Vol 6, Issue 3, pp. 251–260

[18] De Riccardis, M.F., Carbone, D., Rizoo, A., 2007. A novel method for preparing and characterizing alcoholic EPD suspensions, Journal of Colloid and Interface Science, Vol. 307, pp.109–115.

[19] De Beer, E., Duval, J., Meulenkamp, E.A., 2000. Electrophoretic deposition: A quantitative model for particle deposition and binder formation from alcohol-based suspensions, Journal of Colloid and Interface Science, Vol. 222, pp. 117-124.

[20] I. Zhitomirsky, I., Petric, A., 2000. Electrophoretic deposition of ceramic materials for fuel cell applications, Journal of the European Ceramic Society, Vol. 20, pp. 2055-2061.

[21] Li, Z., Qian, S., Wang, W., 2011. Characterization and oxidation behavior of NiCoCrAlY coating fabricated by electrophoretic deposition and vacuum heat treatment, Applied Surface Science, Vol 257, pp.4616–4620.

[22] Wang, Z., Shemilt, J., Xiao, P., 2002. Fabrication of ceramic composite coatings using electrophoretic deposition, reaction bonding and low temperature sintering, Journal of the European Ceramic Society, Vol.22, pp. 183–189.

[23] Van der Biest, O.O., Vandeperre, L.J., 1999. Electrophoretic deposition of materials, Annu. Rev. Mater. Sci., Vol 29, pp.327–352.

[24] Zarbov, M., Brandon, D., Gal-Or, L., Cohen, N., 2006. EPD of metallic silver particles: problems and solutions, Key Engineering Materials, Vol 314, pp. 95-100.

[25] Hosseinbabaei, F., Raissidehkordi, B., 2000. Electrophoretic deposition of MgO thick films from an acetone suspension, Journal of the European Ceramic Society, Vol. 20, Issue 12, pp. 2165–2168.

[26] Corni, I., Ryan, M.P., Boccaccini, A.R., 2008. Electrophoretic deposition: from traditional ceramics to nanotechnology, Journal of the European Ceramic Society, Vol. 28, Issue 7, pp. 1353–1367.

[27] Ferrari, B., Sánchez-Herencia, A.J., Moreno, R., 1998. Aqueous electrophoretic deposition of AL_2O_3/ZrO_2 layered ceramics, Materials Letters, Vol. 35, Issues 5–6, pp. 370–374.

[28] Koura, N., Tsukamoto, T., Shoji, H., Hotta, T., 1995. Preparation of various oxide films by an electrophoretic deposition method: A study of the mechanism, Jpn. J. Appl. Phys., Vol. 34, pp. 1643-1647.

[29] Jean, J-H., 1995. Electrophoretic deposition of Al_2O_3-SiC composite, Materials Chemistry and Physics, Vol. 40, Issue 4, pp. 285–290.

[30] Zhitomirsky, I., Petric, A., 2001. Electrochemical deposition of ceria and doped ceria films, Ceramics International, Vol 27, pp. 149-155

[31] Annal Therese, G.H., Visshnukamath, P., 1998. Cathodic reduction of different metal salt solutions Part I: synthesis of metal hydroxides by electrogeneration of base, Journal of Applied Electrochemistry, Vol28, pp. 539-543.

[32] Xinyi Zhanga, X., Yao. B., Zhao, L., Liang, C., Zhang, L., Mao, Y., 2011. Electrochemical fabrication of single-crystalline anatase TiO_2 nanowire arrays, J. Electrochem. Soc., Vol 148, issue 7, pp.398-400.

[33] Hill, L.I., Portal, R., Verbaere, A., Guyomard, D., 2011. One-step electrochemical synthesis of α-MnO_2 and $\alpha \cdot \gamma$-MnO_2 compounds for lithium batteries, Electrochem. Solid-State Lett. , Vol. 4, issue 11, pp.180-183.

[34] Zhitomirsky, I., Petric, A., 2000. Electrolytic deposition of zirconia and zirconia organoceramic composites, Materials Letters, Vol. 46, Isssue 1, pp. 1-6.

[35] Chaim, R., Stark, G., Gal-Or, L., Bestgen, H., 1994. Electrochemical ZrO_2 and Al_2O_3 coatings on SiC substrates, Journal of Materials Science, Vol. 29, Issue 23, pp 6241-6248.

[36] Chaim, R., Silberman, I., Gal-Or, L., 1991. Electrolytic ZrO_2 coatings II. microstructural aspects, J. Electrochem. Soc. Vol. 138, issue 7, pp. 1942-1946.

[37] Gal-Or, L., Silberman, I., Chaim, R., 1991. Electrolytic ZrO_2 coatings I. electrochemical aspects, Soc. volume 138, issue 7, 1939-1942.

[38] Li, C-F., Wang, M-J., Ho, W-H. Li, H-N., Yen, S-K., 2011. Effects of electrolytic MgO coating parameters on corrosion resistance of AZ91D magnesium alloy, J. Electrochem. Soc., Vol. 158, issue 2, pp.11-16.

[39] Aries, L., Roy, J., Senocq, F., El Hajjaji, S., 2000. Effect of stabilizing heat treatment on characteristics of electrolytic alumina coating on ferritic stainless steel, Materials and Corrosion, Vol. 51,pp. 496-501.

[40] I. Zhitomirsky, 2003. Electrodeposition of lanthanum hydroxide-polyethylenimine films, Materials Letters, Vol. 57, pp. 3761-3766.

[41] Aries, L., Roy, J., El Hajjaji, S., Alberich, L., Vicente Hernandez, P., 1998. Preparation and high-temperature bahaviour of electrolytic alumina film on Fe-Cr-Al stainless steel, Journal of Materials Science, Vol. 33,pp. 429-433.

[42] Abolmaali, S.B., Talbot, J.B., 1993. Synthesis of superconductive thin films of $YBa_2Cu_3O_{7-x}$ by a nonaqueous electrodeposition process, J. Electrochem. Soc., Vol. 140 , pp. 443-445.

[43] Website, visited on January 2013. http://www.nationalboard.org

[44] Website, visited on January 2013. http://ip.com/patfam/en/3711154

[45] Website, visited on January 2013. http://en.wikipedia.org/

[46] Wranglen, G.,1985. An introduction to corrosion and protection of metals, Chapman and Hall Ltd.

[47] Paunovic, M., 2006. Fundamentals of electrochemical deposition, John Wiley & Sons, Inc. 2nd ed.

[48] Randle, V., Engler, O., 2010. Introduction to texture analysis: macrotexture, microtexture, and orientation mapping, CRC Press, Inc. 2nd ed.

[49] Lin, J., 2005. Effect of texture and microstructure of zirconium alloys on their oxidation and oxide texture, Ph.D. thesis, Department of Mining and Metallurgical Engineering, Mc Gill University.

[50] Website, visited on November 2012. http://www.resmat.com

[51] Ahmed, M.S., Attia, Y.A, 1998. Multi-metal oxide aerogel for capture of pollution gases from air, Applied Thermal Engineering, Vol. 18, pp. 787-797.

[52] Zhu, Y., Wu, G., Zhao, Q., Zhang, Y-H., Xing, G., Li, D., 2009. Anticorrosive magnesium hydroxide coating on AZ31 magnesium alloy by hydrothermal method, Journal of Physics: Conference Series, Vol. 188, No. 1.

[53] Walter, M.D., Wajer, M.T., Overview of flame retardants including magnesium hydroxide, Scientific Report by Martin Marietta Magnesia Specialties, LLC.

[54] Maret, M., Saubat, B., Flock,6 J., Mantoux, A., Charlot, F., Makarov, D., 2010. Horizontal single-walled carbon nanotubes on MgO (110) and MgO (001) substrates, Journal of Chemical Physics Letters, Vol. 495, pp. 96-101.

[55] Website, visited on September 2012. http://www.mt-berlin.com.

[56] Bera, P., Rajamathi, M., Hegde, M.S., Kamath, P.V., 2000. Thermal behaviour of hydroxides, hydroxysalts and hydrotalcites, Bull. Mater. Sci., Vol. 23, No. 2, pp. 141–145.

[57] Li, C-F., Ho, W-H., Yen, S-K., 2009. Effects of applied voltage on morphology and crystal orientation of $Mg(OH)_2$ coating on Pt by electrochemical synthesis, Journal of Electrochemical Society, 156 (2), E29-E34.

[58] Website, visited on 11August 201. http://www.azom.com.

[59] Bruker Company, 2005. General area detector diffraction (GADDS), Bruker AXS Inc.

[60] Gond, D., Lalbondre, R.S., Puri, D., Prakash, S., 2012. High temperature oxidation and hot corrosion behaviour of yttria-stabilised zirconia as plasma sprayed coating in air and salt at 900°C under cyclic condition, Technical Applications, Journal of Minerals & Materials Characterization & Engineering, Vol 11, No. 3, pp. 285-302.

[61] Website, visited on December 2012. http://www.hysitron.com

[62] Website, visited on November 2012. http://www.scribd.com/

APPENDIX

This appendix contains the permissions of the figures and tables used in this thesis with the following order:

1- Permission of Figures 2.1, 2.2, 2.3, 2.4

2- Permission of Figure 2.5

3- Permission of Table 2.1

4- Permission of Figures 2.6

5- Permission of Figures 2.7 and 2.8

6- Permission of Figure 3.4

7- Permission of Figure 3.5

JOHN WILEY AND SONS LICENSE TERMS AND CONDITIONS

Jan 15, 2013

This is a License Agreement between Siyamak Javadian ("You") and John Wiley and Sons ("John Wiley and Sons") provided by Copyright Clearance Center ("CCC"). The license consists of your order details, the terms and conditions provided by John Wiley and Sons, and the payment terms and conditions.

All payments must be made in full to CCC. For payment instructions, please see information listed at the bottom of this form.

License Number	3070371357709
License date	Jan 15, 2013
Licensed content publisher	John Wiley and Sons
Licensed content publication	Wiley Books
Book title	None
Licensed content author	Milan Paunovic, Mordechay Schlesinger
Licensed content date	Jul 1, 2006
Type of use	Dissertation/Thesis
Requestor type	University/Academic
Format	Print and electronic
Portion	Figure/table
Number of figures/tables	5
Original Wiley figure/table number(s)	Figure 2.1 Figure 2.12 Figure 4.2 Figure 4.4 Figure 7.18
Will you be translating?	No
Order reference number	None
Total	**0.00 USD**
Terms and Conditions	

TERMS AND CONDITIONS

This copyrighted material is owned by or exclusively licensed to John Wiley & Sons, Inc. or one of its group companies (each a "Wiley Company") or a society for whom a Wiley Company has exclusive publishing rights in relation to a particular journal (collectively WILEY"). By clicking "accept" in connection with completing this licensing transaction, you agree that the following terms and conditions apply to this transaction (along with the billing and payment terms and conditions established by the Copyright Clearance Center Inc., ("CCC's Billing and Payment terms and conditions"), at the time that you opened your Rightslink account (these are available at any time at http://myaccount.copyright.com)

Terms and Conditions

1. The materials you have requested permission to reproduce (the "Materials") are protected by copyright.

2. You are hereby granted a personal, non-exclusive, non-sublicensable, non-transferable, worldwide, limited license to reproduce the Materials for the purpose specified in the licensing process. This license is for a one-time use only with a maximum distribution equal to the number that you identified in the licensing process. Any form of republication granted by this licence must be completed within two years of the date of the grant of this licence (although copies prepared before may be distributed thereafter). The Materials shall not be used in any other manner or for any other purpose.

Permission is granted subject to an appropriate acknowledgement given to the author, title of the material/book/journal and the publisher. You shall also duplicate the copyright notice that appears in the Wiley publication in your use of the Material. Permission is also granted on the understanding that nowhere in the text is a previously published source acknowledged for all or part of this Material. Any third party material is expressly excluded from this permission.

3. With respect to the Materials, all rights are reserved. Except as expressly granted by the terms of the license, no part of the Materials may be copied, modified, adapted (except for minor reformatting required by the new Publication), translated, reproduced, transferred or distributed, in any form or by any means, and no derivative works may be made based on the Materials without the prior permission of the respective copyright owner. You may not alter, remove or suppress in any manner any copyright, trademark or other notices displayed by the Materials. You may not license, rent, sell, loan, lease, pledge, offer as security, transfer or assign the Materials, or any of the rights granted to you hereunder to any other person.

4. The Materials and all of the intellectual property rights therein shall at all times remain the exclusive property of John Wiley & Sons Inc or one of its related companies (WILEY) or their respective licensors, and your interest therein is only that of having possession of and the right to reproduce the Materials pursuant to Section 2 herein during the continuance of this Agreement. You agree that you own no right, title or interest in or to the Materials or any of the intellectual property rights therein. You shall have no rights hereunder other than the license as provided for above in Section 2. No right, license or interest to any trademark, trade name, service mark or other branding ("Marks") of WILEY or its licensors is granted hereunder, and you agree that you shall not assert any such right, license or interest with respect thereto.

5. NEITHER WILEY NOR ITS LICENSORS MAKES ANY WARRANTY OR REPRESENTATION OF ANY KIND TO YOU OR ANY THIRD PARTY, EXPRESS, IMPLIED OR STATUTORY, WITH RESPECT TO THE MATERIALS OR THE ACCURACY OF ANY INFORMATION CONTAINED IN THE MATERIALS, INCLUDING, WITHOUT LIMITATION, ANY IMPLIED WARRANTY OF MERCHANTABILITY, ACCURACY, SATISFACTORY QUALITY, FITNESS FOR A PARTICULAR PURPOSE, USABILITY, INTEGRATION OR NON-INFRINGEMENT AND ALL SUCH WARRANTIES ARE HEREBY EXCLUDED BY WILEY AND ITS LICENSORS AND WAIVED BY YOU.

6. WILEY shall have the right to terminate this Agreement immediately upon breach of this Agreement by you.

7. You shall indemnify, defend and hold harmless WILEY, its Licensors and their respective directors, officers, agents and employees, from and against any actual or threatened claims, demands, causes of action or proceedings arising from any breach of this Agreement by you.

8. IN NO EVENT SHALL WILEY OR ITS LICENSORS BE LIABLE TO YOU OR ANY OTHER PARTY OR ANY OTHER PERSON OR ENTITY FOR ANY SPECIAL, CONSEQUENTIAL, INCIDENTAL, INDIRECT, EXEMPLARY OR PUNITIVE DAMAGES, HOWEVER CAUSED, ARISING OUT OF OR IN CONNECTION WITH THE DOWNLOADING, PROVISIONING, VIEWING OR USE OF THE MATERIALS REGARDLESS OF THE FORM OF ACTION, WHETHER FOR BREACH OF CONTRACT, BREACH OF WARRANTY, TORT, NEGLIGENCE, INFRINGEMENT OR OTHERWISE (INCLUDING, WITHOUT LIMITATION, DAMAGES BASED ON LOSS OF PROFITS, DATA, FILES, USE, BUSINESS OPPORTUNITY OR CLAIMS OF THIRD PARTIES), AND WHETHER OR NOT THE PARTY HAS BEEN ADVISED OF THE POSSIBILITY OF SUCH DAMAGES. THIS LIMITATION SHALL APPLY NOTWITHSTANDING ANY FAILURE OF ESSENTIAL PURPOSE OF ANY LIMITED REMEDY PROVIDED HEREIN.

9. Should any provision of this Agreement be held by a court of competent jurisdiction to be illegal, invalid, or unenforceable, that provision shall be deemed amended to achieve as nearly as possible the same economic effect as the original provision, and the legality, validity and enforceability of the remaining provisions of this Agreement shall not be affected or impaired thereby.

10. The failure of either party to enforce any term or condition of this Agreement shall not constitute a waiver of either party's right to enforce each and every term and condition of this Agreement. No breach under this agreement shall be deemed waived or excused by either party unless such waiver or consent is in writing signed by the party granting such waiver or consent. The waiver by or consent of a party to a breach of any provision of this Agreement shall not operate or be construed as a waiver of or consent to any other or subsequent breach by such other party.

11. This Agreement may not be assigned (including by operation of law or otherwise) by you without WILEY's prior written consent.

12. Any fee required for this permission shall be non-refundable after thirty (30) days from receipt.

13. These terms and conditions together with CCC's Billing and Payment terms and conditions (which are incorporated herein) form the entire agreement between you and WILEY concerning this licensing transaction and (in the absence of fraud) supersedes all prior agreements and representations of the parties, oral or written. This Agreement may not be amended except in writing signed by both parties. This Agreement shall be binding upon and inure to the benefit of the parties' successors, legal representatives, and authorized assigns.

14. In the event of any conflict between your obligations established by these terms and conditions and those established by CCC's Billing and Payment terms and conditions, these terms and conditions shall prevail.

15. WILEY expressly reserves all rights not specifically granted in the combination of (i) the license details provided by you and accepted in the course of this licensing transaction, (ii) these terms and conditions and (iii) CCC's Billing and Payment terms and conditions.

16. This Agreement will be void if the Type of Use, Format, Circulation, or Requestor Type was misrepresented during the licensing process.

17. This Agreement shall be governed by and construed in accordance with the laws of the State of New York, USA, without regards to such state's conflict of law rules. Any legal action, suit or proceeding arising out of or relating to these Terms and Conditions or the breach thereof shall be instituted in a court of competent jurisdiction in New York County in the State of New York in the United States of America and each party hereby consents and submits to the personal jurisdiction of such court, waives any objection to venue in such court and consents to service of process by registered or certified mail, return receipt requested, at the last known address of such party.

Wiley Open Access Terms and Conditions

All research articles published in Wiley Open Access journals are fully open access: immediately freely available to read, download and share. Articles are published under the terms of the Creative Commons Attribution Non Commercial License. which permits use, distribution and reproduction in any medium, provided the original work is properly cited and is not used for commercial purposes. The license is subject to the Wiley Open Access terms and conditions:
Wiley Open Access articles are protected by copyright and are posted to repositories and websites in accordance with the terms of the Creative Commons Attribution Non Commercial License. At the time of deposit, Wiley Open Access articles include all changes made during peer review, copyediting, and publishing. Repositories and websites that host the article are responsible for incorporating any publisher-supplied amendments or retractions issued subsequently.
Wiley Open Access articles are also available without charge on Wiley's publishing platform, **Wiley Online Library** or any successor sites.

Use by non-commercial users

For non-commercial and non-promotional purposes individual users may access, download, copy, display and redistribute to colleagues Wiley Open Access articles, as well as adapt, translate, text- and data-mine the content subject to the following conditions:

- The authors' moral rights are not compromised. These rights include the right of "paternity" (also known as "attribution" - the right for the author to be identified as such) and "integrity" (the right for the author not to have the work altered in such a way that the author's reputation or integrity may be impugned).
- Where content in the article is identified as belonging to a third party, it is the obligation of the user to ensure that any reuse complies with the copyright policies of the owner of that content.
- If article content is copied, downloaded or otherwise reused for non-commercial research and education purposes, a link to the appropriate bibliographic citation (authors, journal, article title, volume, issue, page numbers, DOI and the link to the definitive published version on Wiley Online Library) should be maintained. Copyright notices and disclaimers must not be deleted.
- Any translations, for which a prior translation agreement with Wiley has not been agreed, must prominently display the statement: "This is an unofficial translation of an article that appeared in a Wiley publication. The publisher has not endorsed this translation."

Use by commercial "for-profit" organisations

Use of Wiley Open Access articles for commercial, promotional, or marketing purposes requires further explicit permission from Wiley and will be subject to a fee. Commercial purposes include:

- Copying or downloading of articles, or linking to such articles for further redistribution, sale or licensing;
- Copying, downloading or posting by a site or service that incorporates advertising with such content;
- The inclusion or incorporation of article content in other works or services (other than normal quotations with an appropriate citation) that is then available for sale or licensing, for a fee (for example, a compilation produced for marketing purposes, inclusion in a sales pack)
- Use of article content (other than normal quotations with appropriate citation) by for-profit organisations for promotional purposes
- Linking to article content in e-mails redistributed for promotional, marketing or educational purposes;
- Use for the purposes of monetary reward by means of sale, resale, licence, loan, transfer or other form of commercial exploitation such as marketing products
- Print reprints of Wiley Open Access articles can be purchased from: corporatesales@wiley.com

Other Terms and Conditions:

BY CLICKING ON THE "I AGREE..." BOX, YOU ACKNOWLEDGE THAT YOU HAVE READ AND FULLY UNDERSTAND EACH OF THE SECTIONS OF AND PROVISIONS SET FORTH IN THIS AGREEMENT AND THAT YOU ARE IN AGREEMENT WITH AND ARE WILLING TO ACCEPT ALL OF YOUR OBLIGATIONS AS SET FORTH IN THIS AGREEMENT.

v1.7

If you would like to pay for this license now, please remit this license along with your payment made payable to "COPYRIGHT CLEARANCE CENTER" otherwise you will be invoiced within 48 hours of the license date. Payment should be in the form of a check or money order referencing your account number and this invoice number RLNK500935005. Once you receive your invoice for this order, you may pay your invoice by credit card. Please follow instructions provided at that time.

Make Payment To:
Copyright Clearance Center
Dept 001
P.O. Box 843006
Boston, MA 02284-3006

For suggestions or comments regarding this order, contact RightsLink Customer Support:
customercare@copyright.com or +1-877-622-5543 (toll free in the US) or +1-978-646-2777.

Gratis licenses (referencing $0 in the Total field) are free. Please retain this printable license for your reference. No payment is required.

ELSEVIER LICENSE
TERMS AND CONDITIONS

Oct 23, 2012

This is a License Agreement between Siyamak Javadian ("You") and Elsevier ("Elsevier") provided by Copyright Clearance Center ("CCC"). The license consists of your order details, the terms and conditions provided by Elsevier, and the payment terms and conditions.

All payments must be made in full to CCC. For payment instructions, please see information listed at the bottom of this form.

Supplier	Elsevier Limited The Boulevard,Langford Lane Kidlington,Oxford,OX5 1GB,UK
Registered Company Number	1982084
Customer name	Siyamak Javadian
Customer address	Po Box 443 Saskatoon, SK S7N4J8
License number	3014971054759
License date	Oct 23, 2012
Licensed content publisher	Elsevier
Licensed content publication	Electrochimica Acta
Licensed content title	Elektrochemisch-morphologische studien zur erforschung des mechanismus der elektrokristallisation, fern vom anfangszustand
Licensed content author	H. Seiter,H. Fischer,L. Albert
Licensed content date	February 1960
Licensed content volume number	2
Licensed content issue number	1–3
Number of pages	24
Start Page	97
End Page	120
Type of Use	reuse in a thesis/dissertation
Intended publisher of new work	other
Portion	figures/tables/illustrations
Number of figures/tables/illustrations	1
Format	both print and electronic

Are you the author of this Elsevier article?	No
Will you be translating?	No
Order reference number	
Title of your thesis/dissertation	Electrolytic Deposition of MgO on Stainless Steel Substrate
Expected completion date	Jan 2013
Estimated size (number of pages)	80
Elsevier VAT number	GB 494 6272 12
Permissions price	0.00 USD
VAT/Local Sales Tax	0.0 USD / 0.0 GBP
Total	0.00 USD
Terms and Conditions	

INTRODUCTION

1. The publisher for this copyrighted material is Elsevier. By clicking "accept" in connection with completing this licensing transaction, you agree that the following terms and conditions apply to this transaction (along with the Billing and Payment terms and conditions established by Copyright Clearance Center, Inc. ("CCC"), at the time that you opened your Rightslink account and that are available at any time at http://myaccount.copyright.com).

GENERAL TERMS

2. Elsevier hereby grants you permission to reproduce the aforementioned material subject to the terms and conditions indicated.

3. Acknowledgement: If any part of the material to be used (for example, figures) has appeared in our publication with credit or acknowledgement to another source, permission must also be sought from that source. If such permission is not obtained then that material may not be included in your publication/copies. Suitable acknowledgement to the source must be made, either as a footnote or in a reference list at the end of your publication, as follows:

"Reprinted from Publication title, Vol /edition number, Author(s), Title of article / title of chapter, Pages No., Copyright (Year), with permission from Elsevier [OR APPLICABLE SOCIETY COPYRIGHT OWNER]." Also Lancet special credit - "Reprinted from The Lancet, Vol. number, Author(s), Title of article, Pages No., Copyright (Year), with permission from Elsevier."

4. Reproduction of this material is confined to the purpose and/or media for which permission is hereby given.

5. Altering/Modifying Material: Not Permitted. However figures and illustrations may be altered/adapted minimally to serve your work. Any other abbreviations, additions, deletions and/or any other alterations shall be made only with prior written authorization of Elsevier Ltd. (Please contact Elsevier at permissions@elsevier.com)

6. If the permission fee for the requested use of our material is waived in this instance, please be advised that your future requests for Elsevier materials may attract a fee.

7. Reservation of Rights: Publisher reserves all rights not specifically granted in the combination of (i) the license details provided by you and accepted in the course of this licensing transaction, (ii) these terms and conditions and (iii) CCC's Billing and Payment terms and conditions.

8. License Contingent Upon Payment: While you may exercise the rights licensed immediately upon issuance of the license at the end of the licensing process for the transaction, provided that you have disclosed complete and accurate details of your proposed use, no license is finally effective unless and until full payment is received from you (either by publisher or by CCC) as provided in CCC's Billing and Payment terms and conditions. If full payment is not received on a timely basis, then any license preliminarily granted shall be deemed automatically revoked and shall be void as if never granted. Further, in the event that you breach any of these terms and conditions or any of CCC's Billing and Payment terms and conditions, the license is automatically revoked and shall be void as if never granted. Use of materials as described in a revoked license, as well as any use of the materials beyond the scope of an unrevoked license, may constitute copyright infringement and publisher reserves the right to take any and all action to protect its copyright in the materials.

9. Warranties: Publisher makes no representations or warranties with respect to the licensed material.

10. Indemnity: You hereby indemnify and agree to hold harmless publisher and CCC, and their respective officers, directors, employees and agents, from and against any and all claims arising out of your use of the licensed material other than as specifically authorized pursuant to this license.

11. No Transfer of License: This license is personal to you and may not be sublicensed, assigned, or transferred by you to any other person without publisher's written permission.

12. No Amendment Except in Writing: This license may not be amended except in a writing signed by both parties (or, in the case of publisher, by CCC on publisher's behalf).

13. Objection to Contrary Terms: Publisher hereby objects to any terms contained in any purchase order, acknowledgment, check endorsement or other writing prepared by you, which terms are inconsistent with these terms and conditions or CCC's Billing and Payment terms and conditions. These terms and conditions, together with CCC's Billing and Payment terms and conditions (which are incorporated herein), comprise the entire agreement between you and publisher (and CCC) concerning this licensing transaction. In the event of any conflict between your obligations established by these terms and conditions and those established by CCC's Billing and Payment terms and conditions, these terms and conditions shall control.

14. Revocation: Elsevier or Copyright Clearance Center may deny the permissions described in this License at their sole discretion, for any reason or no reason, with a full refund payable to you. Notice of such denial will be made using the contact information provided by you. Failure to receive such notice will not alter or invalidate the denial. In no event will Elsevier or Copyright Clearance Center be responsible or liable for any costs, expenses or damage incurred by you as a result of a denial of your permission request, other than a refund of the amount(s) paid by you to

Elsevier and/or Copyright Clearance Center for denied permissions.

LIMITED LICENSE

The following terms and conditions apply only to specific license types:

15. **Translation**: This permission is granted for non-exclusive world **English** rights only unless your license was granted for translation rights. If you licensed translation rights you may only translate this content into the languages you requested. A professional translator must perform all translations and reproduce the content word for word preserving the integrity of the article. If this license is to re-use 1 or 2 figures then permission is granted for non-exclusive world rights in all languages.

16. **Website**: The following terms and conditions apply to electronic reserve and author websites:
Electronic reserve: If licensed material is to be posted to website, the web site is to be password-protected and made available only to bona fide students registered on a relevant course if:
This license was made in connection with a course,
This permission is granted for 1 year only. You may obtain a license for future website posting,
All content posted to the web site must maintain the copyright information line on the bottom of each image,
A hyper-text must be included to the Homepage of the journal from which you are licensing at http://www.sciencedirect.com/science/journal/xxxxx or the Elsevier homepage for books at http://www.elsevier.com , and
Central Storage: This license does not include permission for a scanned version of the material to be stored in a central repository such as that provided by Heron/XanEdu.

17. **Author website** for journals with the following additional clauses:

All content posted to the web site must maintain the copyright information line on the bottom of each image, and the permission granted is limited to the personal version of your paper. You are not allowed to download and post the published electronic version of your article (whether PDF or HTML, proof or final version), nor may you scan the printed edition to create an electronic version.
A hyper-text must be included to the Homepage of the journal from which you are licensing at http://www.sciencedirect.com/science/journal/xxxxx . As part of our normal production process, you will receive an e-mail notice when your article appears on Elsevier's online service ScienceDirect (www.sciencedirect.com). That e-mail will include the article's Digital Object Identifier (DOI). This number provides the electronic link to the published article and should be included in the posting of your personal version. We ask that you wait until you receive this e-mail and have the DOI to do any posting.

Central Storage: This license does not include permission for a scanned version of the material to be stored in a central repository such as that provided by Heron/XanEdu.

18. **Author website** for books with the following additional clauses:
Authors are permitted to place a brief summary of their work online only.
A hyper-text must be included to the Elsevier homepage at http://www.elsevier.com . All content

ELSEVIER LICENSE
TERMS AND CONDITIONS

Oct 23, 2012

This is a License Agreement between Siyamak Javadian ("You") and Elsevier ("Elsevier") provided by Copyright Clearance Center ("CCC"). The license consists of your order details, the terms and conditions provided by Elsevier, and the payment terms and conditions.

All payments must be made in full to CCC. For payment instructions, please see information listed at the bottom of this form.

Supplier	Elsevier Limited The Boulevard,Langford Lane Kidlington,Oxford,OX5 1GB,UK
Registered Company Number	1982084
Customer name	Siyamak Javadian
Customer address	Po Box 443 Saskatoon, SK S7N4J8
License number	3014960641328
License date	Oct 23, 2012
Licensed content publisher	Elsevier
Licensed content publication	Applied Thermal Engineering
Licensed content title	Multi-metal oxide aerogel for capture of pollution gases from air
Licensed content author	M.S. Ahmed,Y.A. Attia
Licensed content date	1 September 1998
Licensed content volume number	18
Licensed content issue number	9–10
Number of pages	11
Start Page	787
End Page	797
Type of Use	reuse in a thesis/dissertation
Portion	figures/tables/illustrations
Number of figures/tables/illustrations	1
Format	both print and electronic
Are you the author of this Elsevier article?	No
Will you be translating?	No

Order reference number

Title of your thesis/dissertation	Electrolytic Deposition of MgO on Stainless Steel Substrate
Expected completion date	Jan 2013
Estimated size (number of pages)	80
Elsevier VAT number	GB 494 6272 12
Permissions price	0.00 USD
VAT/Local Sales Tax	0.0 USD / 0.0 GBP
Total	0.00 USD

Terms and Conditions

INTRODUCTION

1. The publisher for this copyrighted material is Elsevier. By clicking "accept" in connection with completing this licensing transaction, you agree that the following terms and conditions apply to this transaction (along with the Billing and Payment terms and conditions established by Copyright Clearance Center, Inc. ("CCC"), at the time that you opened your Rightslink account and that are available at any time at http://myaccount.copyright.com).

GENERAL TERMS

2. Elsevier hereby grants you permission to reproduce the aforementioned material subject to the terms and conditions indicated.

3. Acknowledgement: If any part of the material to be used (for example, figures) has appeared in our publication with credit or acknowledgement to another source, permission must also be sought from that source. If such permission is not obtained then that material may not be included in your publication/copies. Suitable acknowledgement to the source must be made, either as a footnote or in a reference list at the end of your publication, as follows:

"Reprinted from Publication title, Vol /edition number, Author(s), Title of article / title of chapter, Pages No., Copyright (Year), with permission from Elsevier [OR APPLICABLE SOCIETY COPYRIGHT OWNER]." Also Lancet special credit - "Reprinted from The Lancet, Vol. number, Author(s), Title of article, Pages No., Copyright (Year), with permission from Elsevier."

4. Reproduction of this material is confined to the purpose and/or media for which permission is hereby given.

5. Altering/Modifying Material: Not Permitted. However figures and illustrations may be altered/adapted minimally to serve your work. Any other abbreviations, additions, deletions and/or any other alterations shall be made only with prior written authorization of Elsevier Ltd. (Please contact Elsevier at permissions@elsevier.com)

6. If the permission fee for the requested use of our material is waived in this instance, please be advised that your future requests for Elsevier materials may attract a fee.

7. Reservation of Rights: Publisher reserves all rights not specifically granted in the combination of (i) the license details provided by you and accepted in the course of this licensing transaction, (ii) these terms and conditions and (iii) CCC's Billing and Payment terms and conditions.

8. License Contingent Upon Payment: While you may exercise the rights licensed immediately upon issuance of the license at the end of the licensing process for the transaction, provided that you have disclosed complete and accurate details of your proposed use, no license is finally effective unless and until full payment is received from you (either by publisher or by CCC) as provided in CCC's Billing and Payment terms and conditions. If full payment is not received on a timely basis, then any license preliminarily granted shall be deemed automatically revoked and shall be void as if never granted. Further, in the event that you breach any of these terms and conditions or any of CCC's Billing and Payment terms and conditions, the license is automatically revoked and shall be void as if never granted. Use of materials as described in a revoked license, as well as any use of the materials beyond the scope of an unrevoked license, may constitute copyright infringement and publisher reserves the right to take any and all action to protect its copyright in the materials.

9. Warranties: Publisher makes no representations or warranties with respect to the licensed material.

10. Indemnity: You hereby indemnify and agree to hold harmless publisher and CCC, and their respective officers, directors, employees and agents, from and against any and all claims arising out of your use of the licensed material other than as specifically authorized pursuant to this license.

11. No Transfer of License: This license is personal to you and may not be sublicensed, assigned, or transferred by you to any other person without publisher's written permission.

12. No Amendment Except in Writing: This license may not be amended except in a writing signed by both parties (or, in the case of publisher, by CCC on publisher's behalf).

13. Objection to Contrary Terms: Publisher hereby objects to any terms contained in any purchase order, acknowledgment, check endorsement or other writing prepared by you, which terms are inconsistent with these terms and conditions or CCC's Billing and Payment terms and conditions. These terms and conditions, together with CCC's Billing and Payment terms and conditions (which are incorporated herein), comprise the entire agreement between you and publisher (and CCC) concerning this licensing transaction. In the event of any conflict between your obligations established by these terms and conditions and those established by CCC's Billing and Payment terms and conditions, these terms and conditions shall control.

14. Revocation: Elsevier or Copyright Clearance Center may deny the permissions described in this License at their sole discretion, for any reason or no reason, with a full refund payable to you. Notice of such denial will be made using the contact information provided by you. Failure to receive such notice will not alter or invalidate the denial. In no event will Elsevier or Copyright Clearance Center be responsible or liable for any costs, expenses or damage incurred by you as a result of a denial of your permission request, other than a refund of the amount(s) paid by you to Elsevier and/or Copyright Clearance Center for denied permissions.

LIMITED LICENSE

The following terms and conditions apply only to specific license types:

15. **Translation**: This permission is granted for non-exclusive world **English** rights only unless your license was granted for translation rights. If you licensed translation rights you may only translate this content into the languages you requested. A professional translator must perform all translations and reproduce the content word for word preserving the integrity of the article. If this license is to re-use 1 or 2 figures then permission is granted for non-exclusive world rights in all languages.

16. **Website**: The following terms and conditions apply to electronic reserve and author websites:
Electronic reserve: If licensed material is to be posted to website, the web site is to be password-protected and made available only to bona fide students registered on a relevant course if:
This license was made in connection with a course,
This permission is granted for 1 year only. You may obtain a license for future website posting,
All content posted to the web site must maintain the copyright information line on the bottom of each image,
A hyper-text must be included to the Homepage of the journal from which you are licensing at http://www.sciencedirect.com/science/journal/xxxxx or the Elsevier homepage for books at http://www.elsevier.com , and
Central Storage: This license does not include permission for a scanned version of the material to be stored in a central repository such as that provided by Heron/XanEdu.

17. **Author website** for journals with the following additional clauses:

All content posted to the web site must maintain the copyright information line on the bottom of each image, and the permission granted is limited to the personal version of your paper. You are not allowed to download and post the published electronic version of your article (whether PDF or HTML, proof or final version), nor may you scan the printed edition to create an electronic version.
A hyper-text must be included to the Homepage of the journal from which you are licensing at http://www.sciencedirect.com/science/journal/xxxxx . As part of our normal production process, you will receive an e-mail notice when your article appears on Elsevier's online service ScienceDirect (www.sciencedirect.com). That e-mail will include the article's Digital Object Identifier (DOI). This number provides the electronic link to the published article and should be included in the posting of your personal version. We ask that you wait until you receive this e-mail and have the DOI to do any posting.

Central Storage: This license does not include permission for a scanned version of the material to be stored in a central repository such as that provided by Heron/XanEdu.

18. **Author website** for books with the following additional clauses:
Authors are permitted to place a brief summary of their work online only.
A hyper-text must be included to the Elsevier homepage at http://www.elsevier.com . All content posted to the web site must maintain the copyright information line on the bottom of each image.
You are not allowed to download and post the published electronic version of your chapter, nor may you scan the printed edition to create an electronic version.

Central Storage: This license does not include permission for a scanned version of the material to be stored in a central repository such as that provided by Heron/XanEdu.

19. **Website** (regular and for author): A hyper-text must be included to the Homepage of the journal from which you are licensing at http://www.sciencedirect.com/science/journal/xxxxx. or for books to the Elsevier homepage at http://www.elsevier.com

20. **Thesis/Dissertation**: If your license is for use in a thesis/dissertation your thesis may be submitted to your institution in either print or electronic form. Should your thesis be published commercially, please reapply for permission. These requirements include permission for the Library and Archives of Canada to supply single copies, on demand, of the complete thesis and include permission for UMI to supply single copies, on demand, of the complete thesis. Should your thesis be published commercially, please reapply for permission.

21. **Other Conditions**:

v1.6

If you would like to pay for this license now, please remit this license along with your payment made payable to "COPYRIGHT CLEARANCE CENTER" otherwise you will be invoiced within 48 hours of the license date. Payment should be in the form of a check or money order referencing your account number and this invoice number RLNK500883071. Once you receive your invoice for this order, you may pay your invoice by credit card. Please follow instructions provided at that time.

Make Payment To:
Copyright Clearance Center
Dept 001
P.O. Box 843006
Boston, MA 02284-3006

For suggestions or comments regarding this order, contact RightsLink Customer Support: customercare@copyright.com or +1-877-622-5543 (toll free in the US) or +1-978-646-2777.

Gratis licenses (referencing $0 in the Total field) are free. Please retain this printable license for your reference. No payment is required.

ELSEVIER LICENSE
TERMS AND CONDITIONS

Dec 13, 2012

This is a License Agreement between Siyamak Javadian ("You") and Elsevier ("Elsevier") provided by Copyright Clearance Center ("CCC"). The license consists of your order details, the terms and conditions provided by Elsevier, and the payment terms and conditions.

All payments must be made in full to CCC. For payment instructions, please see information listed at the bottom of this form.

Supplier	Elsevier Limited The Boulevard,Langford Lane Kidlington,Oxford,OX5 1GB,UK
Registered Company Number	1982084
Customer name	Siyamak Javadian
Customer address	Po Box 443 Saskatoon, SK S7N4J8
License number	3047230309269
License date	Dec 13, 2012
Licensed content publisher	Elsevier
Licensed content publication	Chemical Physics Letters
Licensed content title	Horizontal single-walled carbon nanotubes on MgO(110) and MgO(001) substrates
Licensed content author	Mireille Maret,Bernadette Saubat,Johanna Flock,Arnaud Mantoux,Frédéric Charlot,Denys Makarov
Licensed content date	29 July 2010
Licensed content volume number	495
Licensed content issue number	1–3
Number of pages	6
Start Page	96
End Page	101
Type of Use	reuse in a thesis/dissertation
Intended publisher of new work	other
Portion	figures/tables/illustrations
Number of figures/tables/illustrations	1

Format	both print and electronic
Are you the author of this Elsevier article?	No
Will you be translating?	No
Order reference number	
Title of your thesis/dissertation	Electrolytic Deposition of MgO on Stainless Steel Substrate
Expected completion date	Jan 2013
Estimated size (number of pages)	80
Elsevier VAT number	GB 494 6272 12
Permissions price	0.00 USD
VAT/Local Sales Tax	0.0 USD / 0.0 GBP
Total	0.00 USD
Terms and Conditions	

INTRODUCTION

1. The publisher for this copyrighted material is Elsevier. By clicking "accept" in connection with completing this licensing transaction, you agree that the following terms and conditions apply to this transaction (along with the Billing and Payment terms and conditions established by Copyright Clearance Center, Inc. ("CCC"), at the time that you opened your Rightslink account and that are available at any time at http://myaccount.copyright.com).

GENERAL TERMS

2. Elsevier hereby grants you permission to reproduce the aforementioned material subject to the terms and conditions indicated.

3. Acknowledgement: If any part of the material to be used (for example, figures) has appeared in our publication with credit or acknowledgement to another source, permission must also be sought from that source. If such permission is not obtained then that material may not be included in your publication/copies. Suitable acknowledgement to the source must be made, either as a footnote or in a reference list at the end of your publication, as follows:

"Reprinted from Publication title, Vol /edition number, Author(s), Title of article / title of chapter, Pages No., Copyright (Year), with permission from Elsevier [OR APPLICABLE SOCIETY COPYRIGHT OWNER]." Also Lancet special credit - "Reprinted from The Lancet, Vol. number, Author(s), Title of article, Pages No., Copyright (Year), with permission from Elsevier."

4. Reproduction of this material is confined to the purpose and/or media for which permission is hereby given.

5. Altering/Modifying Material: Not Permitted. However figures and illustrations may be altered/adapted minimally to serve your work. Any other abbreviations, additions, deletions and/or any other alterations shall be made only with prior written authorization of Elsevier Ltd. (Please

contact Elsevier at permissions@elsevier.com)

6. If the permission fee for the requested use of our material is waived in this instance, please be advised that your future requests for Elsevier materials may attract a fee.

7. Reservation of Rights: Publisher reserves all rights not specifically granted in the combination of (i) the license details provided by you and accepted in the course of this licensing transaction, (ii) these terms and conditions and (iii) CCC's Billing and Payment terms and conditions.

8. License Contingent Upon Payment: While you may exercise the rights licensed immediately upon issuance of the license at the end of the licensing process for the transaction, provided that you have disclosed complete and accurate details of your proposed use, no license is finally effective unless and until full payment is received from you (either by publisher or by CCC) as provided in CCC's Billing and Payment terms and conditions. If full payment is not received on a timely basis, then any license preliminarily granted shall be deemed automatically revoked and shall be void as if never granted. Further, in the event that you breach any of these terms and conditions or any of CCC's Billing and Payment terms and conditions, the license is automatically revoked and shall be void as if never granted. Use of materials as described in a revoked license, as well as any use of the materials beyond the scope of an unrevoked license, may constitute copyright infringement and publisher reserves the right to take any and all action to protect its copyright in the materials.

9. Warranties: Publisher makes no representations or warranties with respect to the licensed material.

10. Indemnity: You hereby indemnify and agree to hold harmless publisher and CCC, and their respective officers, directors, employees and agents, from and against any and all claims arising out of your use of the licensed material other than as specifically authorized pursuant to this license.

11. No Transfer of License: This license is personal to you and may not be sublicensed, assigned, or transferred by you to any other person without publisher's written permission.

12. No Amendment Except in Writing: This license may not be amended except in a writing signed by both parties (or, in the case of publisher, by CCC on publisher's behalf).

13. Objection to Contrary Terms: Publisher hereby objects to any terms contained in any purchase order, acknowledgment, check endorsement or other writing prepared by you, which terms are inconsistent with these terms and conditions or CCC's Billing and Payment terms and conditions. These terms and conditions, together with CCC's Billing and Payment terms and conditions (which are incorporated herein), comprise the entire agreement between you and publisher (and CCC) concerning this licensing transaction. In the event of any conflict between your obligations established by these terms and conditions and those established by CCC's Billing and Payment terms and conditions, these terms and conditions shall control.

14. Revocation: Elsevier or Copyright Clearance Center may deny the permissions described in this License at their sole discretion, for any reason or no reason, with a full refund payable to you. Notice of such denial will be made using the contact information provided by you. Failure to receive such notice will not alter or invalidate the denial. In no event will Elsevier or Copyright

Clearance Center be responsible or liable for any costs, expenses or damage incurred by you as a result of a denial of your permission request, other than a refund of the amount(s) paid by you to Elsevier and/or Copyright Clearance Center for denied permissions.

LIMITED LICENSE

The following terms and conditions apply only to specific license types:

15. **Translation**: This permission is granted for non-exclusive world **English** rights only unless your license was granted for translation rights. If you licensed translation rights you may only translate this content into the languages you requested. A professional translator must perform all translations and reproduce the content word for word preserving the integrity of the article. If this license is to re-use 1 or 2 figures then permission is granted for non-exclusive world rights in all languages.

16. **Website**: The following terms and conditions apply to electronic reserve and author websites:
Electronic reserve: If licensed material is to be posted to website, the web site is to be password-protected and made available only to bona fide students registered on a relevant course if:
This license was made in connection with a course,
This permission is granted for 1 year only. You may obtain a license for future website posting,
All content posted to the web site must maintain the copyright information line on the bottom of each image,
A hyper-text must be included to the Homepage of the journal from which you are licensing at http://www.sciencedirect.com/science/journal/xxxxx or the Elsevier homepage for books at http://www.elsevier.com , and
Central Storage: This license does not include permission for a scanned version of the material to be stored in a central repository such as that provided by Heron/XanEdu.

17. **Author website** for journals with the following additional clauses:

All content posted to the web site must maintain the copyright information line on the bottom of each image, and the permission granted is limited to the personal version of your paper. You are not allowed to download and post the published electronic version of your article (whether PDF or HTML, proof or final version), nor may you scan the printed edition to create an electronic version.
A hyper-text must be included to the Homepage of the journal from which you are licensing at http://www.sciencedirect.com/science/journal/xxxxx . As part of our normal production process, you will receive an e-mail notice when your article appears on Elsevier's online service ScienceDirect (www.sciencedirect.com). That e-mail will include the article's Digital Object Identifier (DOI). This number provides the electronic link to the published article and should be included in the posting of your personal version. We ask that you wait until you receive this e-mail and have the DOI to do any posting.

Central Storage: This license does not include permission for a scanned version of the material to be stored in a central repository such as that provided by Heron/XanEdu.

18. **Author website** for books with the following additional clauses:

Authors are permitted to place a brief summary of their work online only.
A hyper-text must be included to the Elsevier homepage at http://www.elsevier.com . All content posted to the web site must maintain the copyright information line on the bottom of each image.
You are not allowed to download and post the published electronic version of your chapter, nor may you scan the printed edition to create an electronic version.

Central Storage: This license does not include permission for a scanned version of the material to be stored in a central repository such as that provided by Heron/XanEdu.

19. **Website** (regular and for author): A hyper-text must be included to the Homepage of the journal from which you are licensing at http://www.sciencedirect.com/science/journal/xxxxx. or for books to the Elsevier homepage at http://www.elsevier.com

20. **Thesis/Dissertation**: If your license is for use in a thesis/dissertation your thesis may be submitted to your institution in either print or electronic form. Should your thesis be published commercially, please reapply for permission. These requirements include permission for the Library and Archives of Canada to supply single copies, on demand, of the complete thesis and include permission for UMI to supply single copies, on demand, of the complete thesis. Should your thesis be published commercially, please reapply for permission.

21. **Other Conditions**:

v1.6

If you would like to pay for this license now, please remit this license along with your payment made payable to "COPYRIGHT CLEARANCE CENTER" otherwise you will be invoiced within 48 hours of the license date. Payment should be in the form of a check or money order referencing your account number and this invoice number RLNK500917043. Once you receive your invoice for this order, you may pay your invoice by credit card. Please follow instructions provided at that time.

Make Payment To:
Copyright Clearance Center
Dept 001
P.O. Box 843006
Boston, MA 02284-3006

For suggestions or comments regarding this order, contact RightsLink Customer Support: customercare@copyright.com or +1-877-622-5543 (toll free in the US) or +1-978-646-2777.

Gratis licenses (referencing $0 in the Total field) are free. Please retain this printable license for your reference. No payment is required.

Heather McAlinn

From: Siyamak Javadian [siyamak.javadian@gmail.com]
Sent: Tuesday, October 23, 2012 4:19 PM
To: Copyright
Subject: permission to copy figures

Follow Up Flag: Follow up
Flag Status: Flagged

Dear Sir/Madam,

I am Master's student at University of Saskatchewan. I need permission to use two figures (**Figure 6** and **Figure 8**) from the following paper **to be used in my thesis**. I would be grateful if you would give me the permission as soon as possible.

Journal: Journal of Electrochemical Society, 156 (2) E29-E34 (2009)
[DOI: 10.1149/1.3032174]

The thesis will be printed for my committee members.
Deadline: End of November

Thanks and regards,
Siyamak Javadian

Permission is granted to reproduce the above-referenced material. Please acknowledge the author(s) and publication title of the original material, and include the words: "Reproduced by permission of ECS — The Electrochemical Society."

Nov. 1, 2012
Date

Ann F. Goedkoop, Director of Publications

Search

Gmail by Google

Siyamak Javadian <siyamak.javadian@gmail.com

RE: Customer information request

2 messages

He, Bob <Bob.He@bruker-axs.com> Tue, Dec 4, 2012 at 4:45 PM
To: "siyamak.javadian@gmail.com" <siyamak.javadian@gmail.com>
Cc: "Ress, Heiko" <Heiko.Ress@bruker-axs.com>

Dear Siyamak,

Thanks for using Bruker diffractometer in your research. I give you the permission to use the figures in the GADDS Manual. For your convenience, I also attached the two figures in this email for better quality.

Please let me know if need more helps.

Regards,

Bob

Bob He , Ph.D.
Director of Innovation & Business Development-XRD^2

Bruker AXS Inc.
5465 E. Cheryl Parkway
Madison, WI 53711
US

Phone: 608-276-3086
Fax: 608-276-3015

Bob.He@bruker-axs.com
www.bruker.com

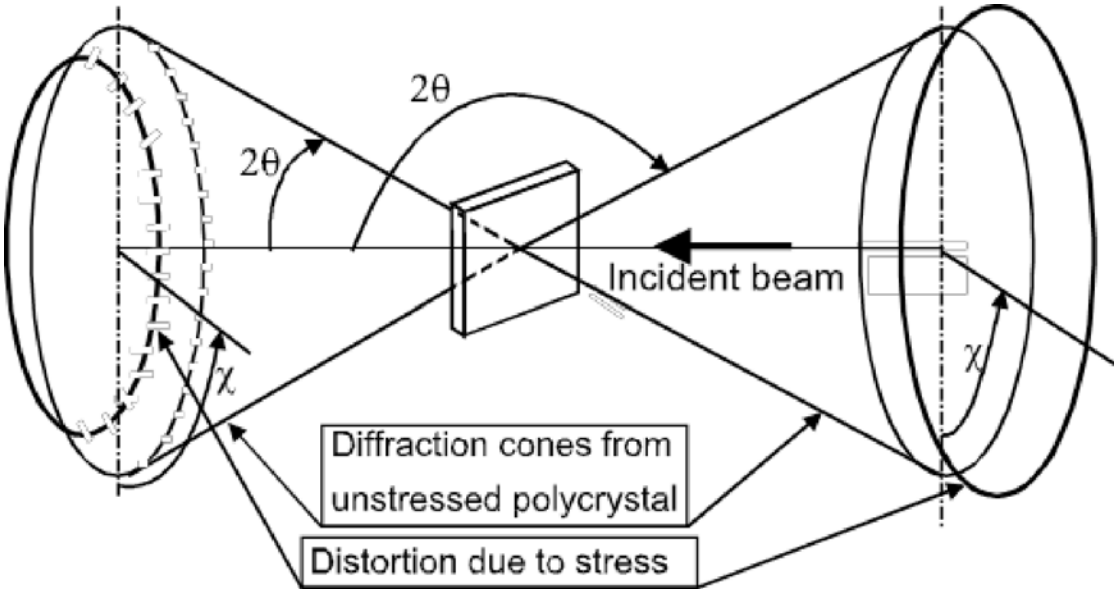

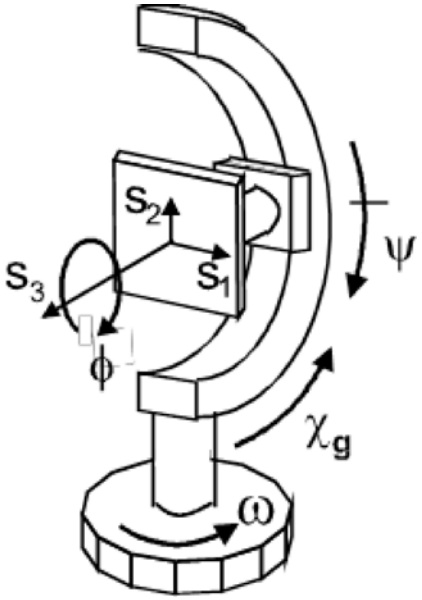

From: Ress, Heiko
Sent: Tuesday, December 04, 2012 4:30 PM
To: He, Bob
Subject: FW: Customer information request

Here's the customer's request, Bob

From: Randell, Amy **On Behalf Of** info
Sent: Tuesday, December 04, 2012 12:26 PM
To: Ress, Heiko
Subject: FW: Customer information request

From: X-ray Diffraction CA [mailto:siyamak.javadian@gmail.com]
Sent: Tuesday, December 04, 2012 12:24 PM
To: Heck, Carina
Subject: Customer information request

Subject:	Question
Technology:	X-ray Diffraction
Industry:	Material Science
First Name:	Siyamak
Last Name:	Javadian
Job Title / Function:	siyamak.javadian@gmail.com
Phone Number:	siyamak.javadian@gmail.com
E-Mail:	siyamak.javadian@gmail.com
Organization:	siyamak.javadian@gmail.com
City:	siyamak.javadian@gmail.com
ZIP Code:	siyamak.javadian@gmail.com
Country:	CA
State (US and CAN only):	SK
Your message:	Dear Sir/Madam, I am doing my Master's at University of Saskatchewan. Our research group isalready using Bruker

XRD and Gadds software. I want to use one of the images in your XRD manual to use it in my thesis. I would be grateful if you would give me the permission to do that. That is figure 6.2 from the manual named (General Area Detector Diffraction System (GADDS) Version 4.1.xx)
Thanks and regards,
Siyamak Javadian

Address:

3 attachments

image001.wmz
13K

image003.wmz
6K

oledata.mso
28K

Siyamak Javadian <siyamak.javadian@gmail.com> Wed, Dec 5, 2012 at 12:18 AM
To: "He, Bob" <Bob.He@bruker-axs.com>

Thank you very much Bob.
[Quoted text hidden]

NANOMECHANICAL
TEST INSTRUMENTS
HYSITRON®

10 December 2012

Siyamak Javadian
University of Saskatchewan
Dept. of Mechanical Engineering
57 Campus Drive
SK, Canada S7N5A9

Dear Siyamak Javadian,

Thank you for your email, requesting authorization to use one of our images located on our website . By this letter, Hysitron is granting you permission for a one-time use of the image shown below, for use specifically in your master's degree thesis at the University of Saskatchewan. Please ensure you label the image with our company name, Hysitron, Inc., as depicted below.

Image Reproduced with Permission from Hysitron, Inc. (Minneapolis, MN)
©Hysitron, Inc.

Best of luck in your research and educational endeavors.

Best Regards,

Oden L. Warren
Chief Technology Officer

cc: A. Hornilla, General Counsel